11

~~P. 100~~

P. 99

(NASA-CR-[illegible]) MICROSTRUCTURAL PROPERTY RELATIONSHIPS IN Al-Cu-Li-Ag-Mg WROUGHT (TM) ALLOYS, PART 2 Final Report, 1 Oct. 1982 - [illegible] Oct. 1988 (Martin Marietta Labs.) [illegible] p

--- N[illegible]
Unclas
CSCL 11F H1/26 0012727

NASA Contractor Report 4364

Microstructure-Property Relationships in Al-Cu-Li-Ag-Mg Weldalite™ Alloys

T. J. Langan and J. R. Pickens
Martin Marietta Corporation
Martin Marietta Laboratories
Baltimore, Maryland

Prepared for
Langley Research Center
under Contract NAS1-18531

National Aeronautics and
Space Administration
Office of Management
Scientific and Technical
Information Division

1991

TABLE OF CONTENTS

P16

EXECUTIVE SUMMARY

A. INTRODUCTION

This document reports the results of research on NASA Contract No. NAS1-18531 during the period October 1, 1988 through October 1, 1990. The goals of the research during this phase of the program were twofold. The first being to investigate microstructure-property relationships in Weldalite™ 049 and modifications of the alloy to assess the effect of increased lithium content. Specifically, microstructural features were related to tensile strength, weldability, Young's modulus, and fracture toughness. The second goal was to evaluate properties of Weldalite™ 049 reinforced with TiB_2 particles fabricated using the XD™ process. An experimental alloy, similar in composition to Weldalite™ 049, but without the Ag+Mg, was also fabricated. The microstructure of this alloy was compared with that of Weldalite™ 049 in the T6 condition to assess the effect of Ag+Mg on nucleation of strengthening phases in the absence of cold-work. The results of all this research are summarized here and are discussed in detail in Sections II, III and IV and Appendices A,B, and C.

B. MATERIAL FABRICATION

The initial composition of Weldalite™ 049 -- Al-6.3Cu-1.3Li-0.4Ag-0.4Mg-0.14Zr -- was designed to have a high Cu content to ensure good weldability. Consequently, the experimental alloys investigated during this first year of the program had high copper contents. Subsequent research at both Martin Marietta Laboratories and Martin Marietta's operating companies showed that good weldability could be obtained at lower Cu levels -- down to 4.75 wt% -- with no loss in tensile strength, yet significant improvements in ductility and fracture toughness.

Alloys for this program were fabricated under Martin Marietta funding and provided to NASA for evaluation. Five billets, each weighing 23 kg (50 lb), were cast at Martin Marietta Laboratories in a controlled-atmosphere furnace under an Ar cover. After casting, the billets were homogenized, scalped, and shipped to International Light Metals, Torrance, CA, for extrusion. The 15.6-cm (6.13-in)-diameter billets were extruded into 0.95 x 10.2-cm (0.375 x 4-in.) bars in a 16.2-cm (6.38-in.) container, at an extrusion ratio of about 20 to 1. After extrusion, the bars were solution-heat-treated, water quenched and stretched as indicated in Table I.

TABLE I

Alloy	Solution Heat Treatment Temperature °C	(°F)	/ Time (min)	% Stretch for T3 and T8 Tempers
049(1.3)				
heat 072	504	(940)	60	3½
heat 116	504	(940)	60	3½
049(1.6)	493	(920)	200	3
049(1.9)	493	(920)	200	3
049-TiB_2	504	(940)	60	2½*
049[OAg+OMg]	504	(940)	60	NA

*Broke on stretching

The nominal Weldalite™ 049 alloy composition studied was Al-6.3Cu-xLi-0.4Mg-0.4Ag-0.14Zr, where x varied from 1.3 to 1.9 wt%, nominal. Alloys evaluated are identified as 049(x), where x represents the Li content in wt%. Two different heats of 049(1.3) were evaluated, identified as 049(1.3) [heat 072] and 049(1.3) [heat 116]. The model alloy fabricated without the nucleation aids Ag and Mg is referred to as 049[0Ag+0Mg]. Weldalite™ 049(1.3) reinforced with TiB_2 was also evaluated and is referred to as 049-TiB_2. The nominal and measured compositions for these alloys are given in Table II. Impurity levels of Fe and Si measured for alloys 049(1.3) [heat 072] and 049-TiB_2 are representative of levels in all of the alloys.

Hardness as a function of artificial aging at 160°C (i.e., aging curves) was measured after 3% cold stretch to determine the peak-strength condition.[1] For the purpose of this study, the T8 temper was defined as 24 h at 160°C for 049(1.3) and 049(1.3)-TiB_2, and 334 h at 160°C for 049(1.6) and 049(1.9). Based on aging curves developed for unstretched material, the T6 temper was defined as 24 h at 180°C.

C. IDENTIFICATION OF STRENGTHENING PHASES IN Al-Cu-Li ALLOY WELDALITE™ 049

The addition of Li to aluminum alloys decreases density and increases elastic modulus. Thus, increasing the Li content of Weldalite™ 049 should improve specific stiffness, but, as was first shown by Pickens et al. [1], increasing the Li content above about 1.3 wt% decreases the alloy's strength. To

1) J.R. Pickens, F.H. Heubaum, L.S. Kramer, and K.S. Kumar, U.S. Patent Application Serial No. 07/327,927 Filed March 23, 1989 which is a Continuation-in-Part (CIP) of Serial No. 083,333 Filed August 10, 1987.

TABLE II

Nominal and Measured Alloy Compositions (wt%)

Alloy	Cu	Li	Mg	Ag	Zr	Ti	B	Fe	Si
049(1.3) nominal	6.30	1.30	0.40	0.40	0.14	--	--	--	--
[heat 072] measured	5.85	1.25	0.43	0.38	0.14	--	--	0.03	0.02
049(1.3) nominal	6.30	1.30	0.40	0.40	0.14	0.01	--	--	--
[heat 116] measured	6.13	1.11	0.37	0.38	0.15	0.04	--	--	--
049(1.6) nominal	6.30	1.60	0.40	0.40	0.14	--	--	--	--
measured	6.29	1.62	0.49	0.41	0.14	--	--	--	--
049(1.9) nominal	6.30	1.90	0.40	0.40	0.14	--	--	--	--
measured	6.32	1.86	0.46	0.41	0.14	--	--	--	--
049-TiB_2 nominal	6.30	1.30	0.40	0.40	0.14	--	--	--	--
measured*	6.28	1.38	0.42	0.34	0.15	4.58-3.90	1.65-1.89	0.06	0.02
049[0Ag+0Mg] nominal	6.30	1.30	-	-	0.14	--	--	--	--
measured	5.83	1.25	-	-	0.14	--	--	--	--

* Some variability was observed in the Ti and B controls, possibly due to the nonuniform distribution of the TiB_2 particles.

elucidate the cause of this decrease in strength, we investigated the strengthening phases present in 049(1.3)[heat 072] and 049(1.9) using conventional transmission electron microscopy and high-resolution transmission electron microscopy (HRTEM).

Electron diffraction results from 049(1.3)[heat 072] in the T8 temper, i.e., 24 h at 160°C, show that the primary strengthening phase is a T_1-type precipitate with a {111} habit plane. This phase is referred to as T_1-type because of difficulties in unambiguously indexing it as the T_1-phase (Al_2CuLi) or as the Ω-phase (observed by Chester and Polmear[2] in Al-Cu-Mg-Ag alloys) due to similarities electron diffraction from the two phases. Preliminary HRTEM of the T_1-type phase in 049(1.3)[heat 072] shows that its structure is similar to that of the T_1 phase observed in 2090. Since the T_1 phase is associated with high strengths in Al-Cu-Li alloys, the presence of homogeneously distributed T_1-type platelets as the only major strengthening phase in 049(1.3)[heat 072] can qualitatively explain the alloys' ultra-high strength. (Minor amounts of θ' ($CuAl_2$) have been observed in some, but not all, specimens in this aging condition.)

Alloy 049(1.9) is strengthened by a combination of the T_1-type precipitates, the δ'-phase (Al_3Li) and the θ'-phase (Al_2Cu). It was speculated that the precipitation of δ' and θ' may decrease the volume fraction or effectiveness of the T_1-type precipitates and result in a decrease in strength.

2) R.J. Chester and I.J. Polmear, The Metallurgy of Light Alloys, Inst. of Metals, London, pp. 75-81 (1983).

D. THE INFLUENCE OF Ag+Mg ADDITION ON THE NUCLEATION OF STRENGTHENING PRECIPITATES IN AN Al-Cu-Li ALLOY IN THE ABSENCE OF STRETCH

Pickens and coworkers [3,4] showed that the tensile strength of Weldalite™ 049 exceeds 100 ksi both with and without prior cold work (i.e., stretch) in artificially aged tempers. This is a unique property for an Al-Cu-Li alloy since cold work is generally required to attain maximum strength. Microstructures of 049(1.3) and a model alloy without the Ag+Mg addition, 049[0Ag+0Mg], were compared in the T6 temper (i.e., unstretched and artificially aged for 24 h at 180°C) to elucidate the role of the Ag+Mg addition in the strengthening of Weldalite™ 049.

Alloy 049[0Ag+0Mg] is strengthened by θ' and T_1 precipitates in the T6 temper, with θ' being the more prevalent strengthening phase. The T_1 precipitates are heterogeneous and surrounded by a θ' precipitate-free zone. Alloy 049(1.3) is strengthened primarily by a uniform distribution of fine T_1-type precipitates. Based on results of selected area electron diffraction, the T_1-type precipitates are the only strengthening phase present in 049(1.3) in this temper (aged at 180°C for 24 h). It is possible that some θ' may be present at a volume fraction which is too low to provide detectable diffraction information. Thus the Ag+Mg addition promotes precipitation of uniform T_1-type precipitates, apparently at the expense of the θ' phase.

3) J.R. Pickens, F.H. Heubaum, T.J. Langan and L.S. Kramer, in Proc. of Fifth Int. Al-Li Conf., T.H. Sanders, and E.A. Starke, Jr., eds., Mater. Component Eng. Publ. Ltd., London (1989)
4) J.R. Pickens, F.H. Heubaum and L.S. Kramer, Scripta Metall., vol. 24, 1990, pp. 457-462.

We propose that the Ag+Mg addition increases the nucleation of T_1-type precipitates by the following mechanism. The high affinity between Mg and vacancies will increase the concentration of quenched-in vacancies, which increases the number of vacancy loops. The vacancy loops would then collapse to form faulted loops which could act as effective nuclei for the precipitation of T_1-type precipitates. These loops are bound by sessile partial dislocations that form without prior cold work, which explains the uniform T_1-type precipitate distribution present in the unstretched artificially aged temper.

E. THE EFFECT OF TiB_2 REINFORCEMENT ON THE MECHANICAL PROPERTIES OF AN Al-Cu-Li ALLOY-BASED METAL-MATRIX COMPOSITE

The goal of this research was to evaluate the room- and elevated-temperature mechanical properties for a Weldalite™ 049 metal-matrix composite (MMC) reinforced with TiB_2 particles fabricated by the XD™ process. A relatively low volume fraction of TiB_2 (~4%) was selected for a preliminary assessment of the viability of such an MMC.

Agglomeration of the TiB_2 particles in the MMC results in a decrease in ductility. This agglomeration occurs during the fabrication of the TiB_2 by the XD™ process and is apparently not related to the Weldalite™ 049 alloy matrix. The reinforced alloy (049-TiB_2) showed a good combination of strength (529 MPa UTS) and ductility (6.5%) in the naturally aged temper even with the agglomerated TiB_2 particles present.

TiB_2 reinforcement at this volume fraction did not increase the tensile strength of Weldalite™ 049, but did produce a slight increase in aging

kinetics, with the time required to reach peak strength decreasing from around 24 h for 049(1.3) to only 10 h in 049-TiB_2. The TiB_2 reinforcement increased Young's Modulus by about 8% to 84.7 GPa (12.3 Msi).

Both the TiB_2-reinforced and non-reinforced alloy variants showed good tensile strengths at warm temperatures. The TiB_2 reinforcement did not improve the elevated-temperature strength or stability of Weldalite™ 049, and the increase in aging kinetics associated with the reinforcement may actually have resulted in a slight decrease in strength after exposures of 100 h.

This preliminary assessment shows that Weldalite™ 049 is a promising candidate for high-strength MMC's that have good warm-temperature properties. Also, once the agglomeration problem is solved, the combination of Weldalite™ 049 with TiB_2 produced by the XD™ process could result in an ultra-high-strength, high-modulus MMC.

F. WELDABILITY OF WELDALITE™ 049 WITH AND WITHOUT TiB_2 REINFORCEMENT

The weldability of Weldalite™ 049 was assessed for alloys 049-TiB_2, 049(1.9) and 049(1.3). Manual gas tungsten arc (GTA) welding was used for the work reported here. An extensive study involving optimization of welding parameters and filler alloy development is currently under way at Martin Marietta Laboratories (funded by Martin Marietta Corporation).

No propensity to hot crack was observed for the 049(1.3) or the 049-TiB_2 weldments. The TiB_2 reinforced weldments were no stronger than those of Weldalite™ 049. Weldment tensile strengths were between ~300 and 317 MPa (44 and 46 ksi) for either reinforced or nonreinforced filler and parent metal.

No hot cracking was observed in the higher lithium-containing unreinforced alloy weldments. Increasing the lithium level from 1.3 to 1.9 wt% in the parent or filler alloy had no effect on weldment strength. A decrease in weldment ductility was associated with higher lithium-containing filler metal.

Weldment tensile strengths obtained for reinforced or nonreinforced Weldalite™ 049 were always higher than the typical values of weldment strength for 2219. This is very encouraging since the welding parameters used here were not optimized. In fact, optimization of welding parameters for Weldalite™ 049 at Martin Marietta Manned Space Systems[5] has resulted in variable polarity plasma arc weldments with a mean strength of 372 MPa (54ksi).

G. EFFECT OF Li CONTENT, ARTIFICIAL AGING, AND TiB_2 REINFORCEMENT ON THE FRACTURE TOUGHNESS OF WELDALITE™ 049

Plane-strain fracture toughness (K_{IC}) was measured for Weldalite™ 049 with and without TiB_2 reinforcement. The K_{IC} values for alloys 049(1.3)[heat 072] and 049-TiB_2 were similar after aging for 24 h at 160°C. The K_{IC} values for 049(1.3)[heat 072] were unexplainably lower than those obtained in other heats of Weldalite™ 049.

Toughness is greatly improved by underaging Al-Cu-Li alloys in general, and this also is the case for Weldalite™ 049. Values of K_{IC} of up to 27.3 MPa $\sqrt{m}$ (24.8 ksi $\sqrt{in}$) were obtained on 049(1.3)[heat 072] after aging for 6 h at 160°C, with a yield strength of 593 MPa (86 ksi). Alloy 049(1.3)[heat 116]

(5) J.R. Pickens, "Recent Developments in Weldability of Lithium-Containing Aluminum Alloys," J. Mater. Sci., Vol. 10, pp. 3035-3047,(1990).

similarly displayed a substantial improvement in toughness on underaging, with a K_{IC} in the T8 temper (20 h at 160°C) of 22.5 MPa $\sqrt{m}$ (20.5 ksi $\sqrt{in}$) at a yield strength of 700 MPa(100 ksi) and a K_{IC} in an underager temper of 35.7 MPa $\sqrt{m}$ (32.5 ksi $\sqrt{in}$) at a yield strength of 565 MPa (82 ksi). The toughness values for 049(1.3)[heat 116] are very good for an aluminum-lithium alloy at this ultra-high strength level. An extensive temper development program at Martin Marietta Laboratories and Reynolds Metal Co. resulted in even further increases in K_{IC} when the Cu content was reduced from 6.3% to 4.75 wt%. A K_{IC} value of 33 MPa $\sqrt{m}$ (30 ksi $\sqrt{in}$) was obtained from commercial plate at this Cu level, with a 625 MPa (90 ksi) yield strength.

A preliminary assessment of the effect of Li level on K_{IC} showed that increasing the Li content decreases K_{IC} for alloys aged to comparable strength levels. A definitive conclusion on the effect of Li level on K_{IC} cannot be drawn because of the relatively low K_{IC} values for 049(1.3)[heat 072] found in the peak-aged temper. Thus, additional data from other alloy heats are needed, coupled with results of studies on the influences of grain boundary (GB) and matrix microstructures.

H. EFFECT OF Li LEVEL, ARTIFICIAL AGING AND TiB_2 REINFORCEMENT ON THE MODULUS OF WELDALITE™ 049

Young's Modulus (E) for alloys 049(1.3)[heat 072], 049(1.9), and 049-TiB_2 was determined by an ultrasonic pulse-echo technique as a function of aging time. Both the high- and low-lithium variants of Weldalite™ 049, 049(1.9), and 049(1.3)[heat 072] showed slight changes in E during artificial aging, which closely mirrored changes in strength observed. The change in E for Weldalite™ 049 is more subtle than that observed in 2090-type alloys.(7) This decreased dependence of E on aging means that Weldalite™ 049 can be used in an underaged temper with only a minor decrease in E.

As expected, increasing the Li level increased E, with 049(1.9) having a 2% higher E than 049(1.3). The observed modulus increase was slightly less than that expected by the general rule of thumb: 1 wt% Li increases E by 6%. The reason for this small deviation is unclear.

TiB_2 reinforcement of Weldalite™ 049 at a nominal 4 vol. % resulted in a 8% increase in E. Further increases in E would accompany higher volume fractions of TiB_2, but the agglomeration of TiB_2 particles must be eliminated before 049-TiB_2 can be a viable structural alloy.

(7) M.E. O'Dowd, W. Buch, and E.A. Starke, Jr., J. Physique (Paris), 48, c3, pp. c-565-576.

I. SUMMARY OF RESULTS

- Weldalite™ 049 is primarily strengthened by a uniform distribution of fine T_1-type precipitates in the T8 temper.

- The decrease in T8 strength with increasing lithium content for Weldalite™ 049-type alloys is associated with precipitation of the $\delta'(Al_3Li)$ phase.

- Preliminary HRTEM shows that the T_1-type precipitates in Weldalite™ 049 T8 are similar in structure to T_1 in 2090.

- The Ag+Mg in Weldalite™ 049 promotes high strength in T6 tempers and eliminates the requirement for cold work to nucleate strengthening precipitates.

- Agglomeration of TiB_2 particles limits the ductility of a Weldalite™ 049-TiB_2 MMC. Nevertheless, promising combinations of strength and ductility are obtained in the T3 and underaged tempers, suggesting that Weldalite™ 049 is a good matrix for ceramic reinforcement.

- Reinforcement with only 4 v% TiB_2 increases E by 8%.

- Weldalite™ 049 and Weldalite™ 049-TiB_2 show very high strength at warm temperatures compared with leading conventional warm-temperature aluminum alloys such as 2219.

- No propensity for hot cracking was observed for Weldalite™ 049 at any lithium level investigated or for Weldalite™ 049-TiB_2.

- Weldment strengths higher than those of 2219 are easily obtained for Weldalite™ 049 with non-optimized welding parameters.

- The toughness of Weldalite™ 049 is low on one heat for unexplained reasons, yet high for another. Yield strength-toughness combinations for the better of the two heats are very encouraging.

- Young's modulus (E) varies only slightly with artificial aging for Weldalite™ 049.

- Increasing the lithium content of Weldalite™ 049 from 1.3 to 1.9 wt% results in only a 1.5 to 2% increase in E.

ACKNOWLEDGEMENTS/CONTRIBUTIONS

This research was sponsored by the NASA Langley Research Center under the auspices of W. Brewer, Contract Monitor. The authors of this report gratefully acknowledge the contributions of the following individuals:

F.H. Heubaum:	Material fabrication
L.S. Kramer:	Welding studies, material fabrication
L. Friant:	Ultrasonic modulus measurement
R. Aikin,	Fabrication of XD™-TiB_2 particles
M. Buchta:	Fabrication of XD™-TiB_2 particles
R. Herring:	High-resolution transmission electron microscopy
K. Moore:	Mechanical testing
W. Precht:	Mechanical testing
J. Doherty:	Welding

We also thank F.W. Gayle, K.S. Kumar, and A.J. Ardell for their insightful comments on the electron microscopy studies.

I. IDENTIFICATION OF STRENGTHENING PHASES IN Al-Cu-Li ALLOY WELDALITE™ 049

IDENTIFICATION OF STRENGTHENING PHASES IN Al-Cu-Li ALLOY WELDALITE™ 049†

Microstructure-property relationships were determined for a family of ultrahigh-strength weldable Al-Cu-Li based alloys, developed at Martin Marietta and referred to as Weldalite™ alloys. The highest strength variant of this family, Weldalite™ 049, has a high Cu/Li wt% ratio with a nominal composition of Al-6.3Cu-1.3Li-0.4Ag-0.4Mg-0.14Zr. Increasing the alloy's lithium content above 1.3 wt% resulted in a decrease in both yield and ultimate tensile strength. Strength was shown to be strongly dependent on lithium content, with a maximum in strength occurring in the range of about 1.1 to 1.4 wt% lithium. The strengthening phases present in Weldalite™ 049 (1.3Li) and an Al-6.3Cu-1.9Li-0.4Ag-0.4Mg-0.14Zr alloy were identified using transmission electron microscopy (TEM).

†Weldalite™ 049 alloys were developed by Martin Marietta Corporation and are used under license from Comalco Aluminum, Ltd.

INTRODUCTION

Weldalite™ 049, a weldable Al-Cu-Li alloy, obtains ultrahigh strength in the T8 temper. The alloy design considerations and resulting properties are discussed by Pickens et al. (1).

The microstructure of Al-Cu-Li alloys was first studied extensively by Hardy and Silcock (2) and then by Silcock (3), who investigated precipitation after artificial aging (3). Work on the recently commercialized Al-Cu-Li alloy 2090 by Rioja and Ludwiczak (4) and Huang and Ardell (5) confirmed the results of Silcock (3), which show that Al-Cu-Li alloys are strengthened primarily by precipitation of T_1 (Al_2CuLi) and/or δ' (Al_3Li) phases. Both Silcock (3) and Rioja and Ludwiczak (4) showed that the metastable δ'-phase was not present if the alloy contained primary $T_B(Al_{7.5}Cu_4Li)$ phase.

Although Weldalite™ 049 is an Al-Cu-Li based alloy, the relatively minor additions of Mg and Ag give it unique properties. Trace addition effects on precipitation in aluminum alloys have been studied extensively by Polmear and coworkers (6-8) with particular emphasis on Mg and Ag additions. They observed a large increase in strength on adding Mg and Ag to an Al-Cu alloy, resulting from precipitation of the so-called Ω-phase with a {111} habit plane, rather than θ*-type† precipitates with a {100} habit plane. The structure of the Ω-phase (9) is very close to that of the T_1-phase, which has been shown to be a very potent strengthener in Al-Cu-Li alloys (10,11).

† θ* represents metastable Al_2Cu precipitates with a {100} habit plane, e.g., θ".

In the work reported here, we assessed the tensile properties in the peak-strength T8 temper for Weldalite™ 049 with a Li content ranging from 0 to 1.9 wt% and identified strengthening precipitates at selected Li levels.

Materials and Experimental Procedures

Weldalite™ 049†† -type alloys with lithium contents ranging from 0-1.9††† wt% were fabricated for evaluation. The compositions are given in Table 1.

Table 1

Chemical composition of Weldalite™ 049 variants with different lithium levels as measured using the inductively coupled plasma technique.

	wt%				
Alloy	Cu	Li	Mg	Ag	Zr
049(0)	6.16	---	0.42	0.41	0.14
049(0.9)	5.82	0.88	0.35	0.39	0.16
049(1.3)	5.85	1.25	0.43	0.38	0.13
049(1.6)	6.29	1.62	0.49	0.41	0.16
049(1.9)	6.32	1.86	0.46	0.41	0.14
2090	2.60	2.20	---	---	0.12

†† Hereafter called 049(wt% Li),e.g., 049(1.3), meaning Weldalite™ 049 with a nomimal 1.3 wt% Li content.

†††Strictly speaking, 049(0) is not a Weldalite™ 049 alloy variant, but since its Cu, Mg, Ag and Zr levels are nominally the same as those in Weldalite™ 049, it will be referred to as 049(0) in this paper. (This alloy is similar to those studied by Polmear.)

Billets weighing 23 kg (50 lb) were cast for each composition using an Ajax vacuum furnace under an Ar cover. The billets were extruded into 9.5-mm x 102-mm (0.375 x 4-in) bar at International Light Metals. Alloys 049(0), 049(0.9), and 049(1.3) were solution heat treated for 1 h at 504°C (940°F), water quenched, and stretched 3.5%; alloys 049(1.6) and 049(1.9) were solution heat treated for 1 h at 493°C (920°F), water quenched, and stretched 3%. Rockwell B hardness (R_B) was measured after various times at 160°C (320°F) to determine peak aging conditions for 049(1.3), 049(1.6), and 049(1.9). Peak aging times of 24 h for 049(1.3) and 34 h for 049(1.6) and 049(1.9) were selected based on hardness data. Alloy 2090 T8E41 was used for comparison in certain cases.

Specimens of selected alloys were examined by transmission electron microscopy (TEM) in a JEOL 100CX at Martin Marietta Laboratories, and by high-resolution TEM (HRTEM) in a Phillips EM430 at the National Institute of Science and Technology in Gaithersburg, MD. Foils were made by jet thinning at -30°C and 11 V in a solution of 75% methanol and 25% nitric acid.

RESULTS

As previously shown (12), Weldalite™ 049 exhibits a strong strength dependence on lithium content (Fig. 1). Note the peak in both ultimate tensile strength (Fig. 1a) and yield strength (Fig. 1b) at lithium levels between 1.0 and 1.4 wt%. The tensile properties for the variants discussed in this paper are given in Table 2.

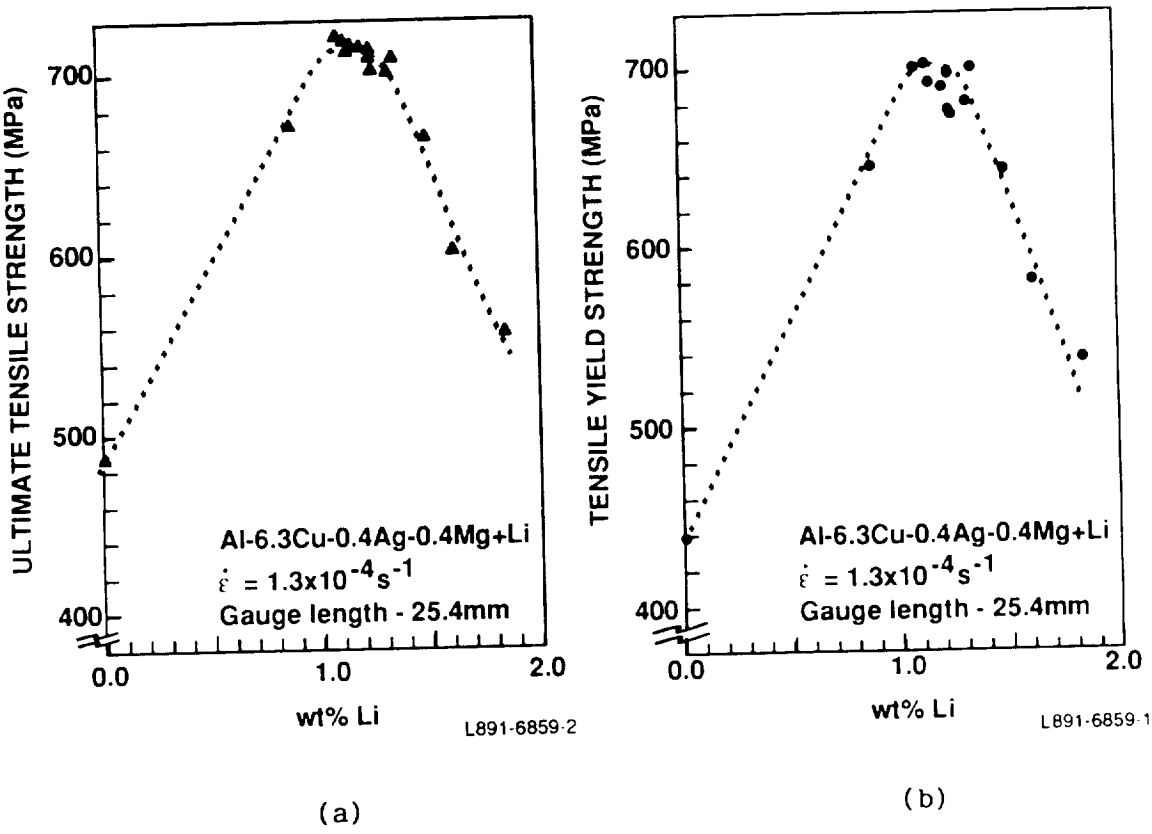

Figure 1. Ultimate tensile strength (a) and yield strength (b) vs. wt% lithium (Ref. 12).

Table 2

Tensile properties for Weldalite™ 049 with four different lithium levels in the T8 temper.

Alloy ID#	Lithium Content wt%	Aging Time h at 160°C	Yield Strength MPa	Ultimate Tensile Strength MPa	Elongation %
049(0)	0.00	24	441	489	12.9
049(1.3)	1.25	24	676	707	3.7
049(1.6)	1.62	34	581	602	5.2
049(1.9)	1.86	34	538	556	3.9

Although a detailed aging study was not performed for 049(0) and 049(0.9), near-peak-aged tensile properties are reported. The data in Fig. 1 and Table 2 clearly indicate that lithium level strongly influences mechanical properties, implying changes in microstructure between 0 and 1.9 wt% lithium. When the compositions of the Weldalite™ 049 variants are plotted on a modified version of Silcock's (3) phase diagram, they fall into four different equilibrium phase fields (Fig. 2). Alloy 049(0) is in an equilibrium two-phase region containing Al_{ss}+θ, and should be strengthened by θ*-type precipitates after artificial aging (3). Alloy 049(0.9) is in an equilibrium two-phase field containing Al_{ss}+T_B. Ternary Al-Cu-Li alloys of this composition were shown by Silcock (3) to be strengthened by θ' after artificial aging. Alloy 049(1.3) falls on the boundary of an equilibrium three-phase field with Al_{ss}+T_B+T_1, and both 049(1.6) and 049(1.9) fall into an equilibrium two-phase field containing Al_{ss}+T_1. Based on their compositions, and Silcock's work, 049(1.3) should be out of, and 049(1.6) and 049(1.9) should be in the metastable δ'-phase field (3,4).

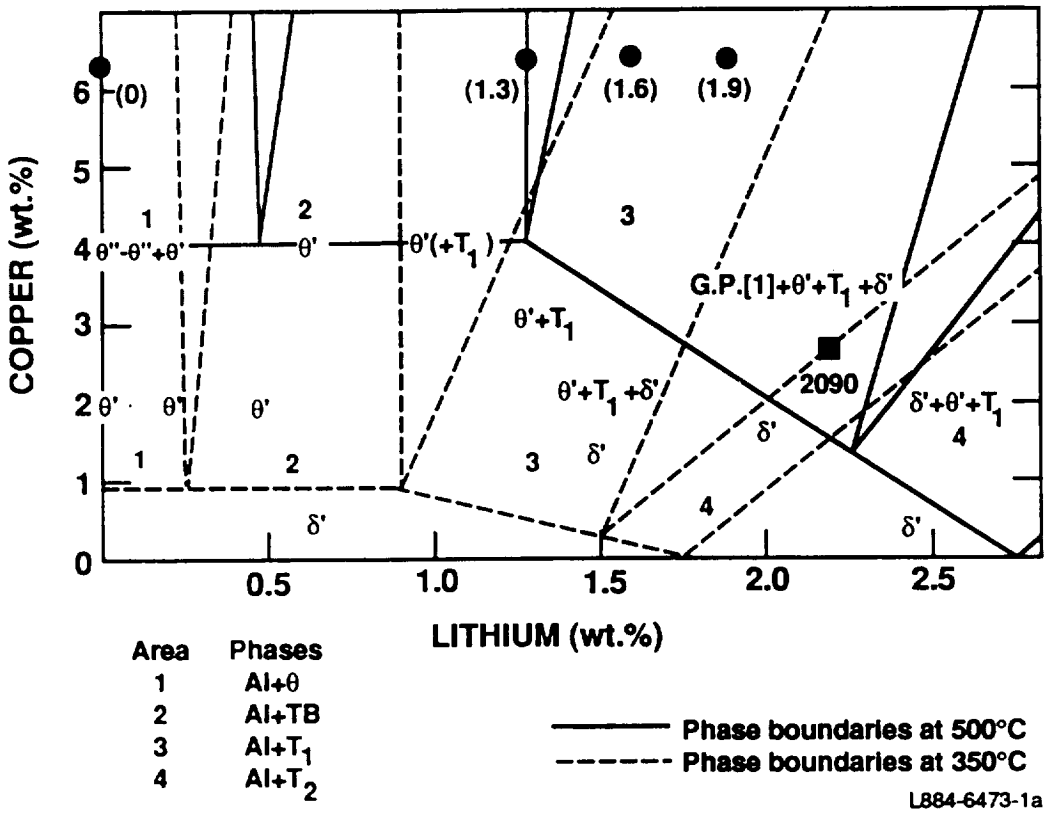

Figure 2. Aluminum corner of the Al-Cu-Li phase diagram (2) with compositions of various Weldalite™ heats. Numbers 1-4 give equilibrium phase relations. Phases observed by Silcock (3), e.g., $\theta' + T_1 + \delta'$, after aging 16 h at 160°C are also shown.

TEM was performed on 049(0), 049(1.3), and 049(1.9) to compare the strengthening phases present in the peak-aged tempers with those observed by Silcock (3) for Al-Cu-Li ternary alloys aged 16 h at 165°C. TEM was also performed on alloy 2090 in the T8E41 temper for comparison purposes. Selected-area electron diffraction (SAD) patterns were indexed for these four alloys with the electron beam direction (B) parallel to the aluminum [112] zone axis (Fig. 3). Reflections from the δ'-phase in 2090 appear in Fig. 3d as the bright spots in the superlattice position (indicated by the arrow), and the diffraction from T_1 appears as streaks due to its platelike morphology. The streaking in 049(0) (Fig. 3a) results from diffraction by Ω platelets. This streaking coincides with the streaking observed in diffraction from the T_1-phase, but cannot be T_1 (Al_2CuLi) since this alloy has no lithium. The SAD pattern for 049(1.3) (Fig. 3c) with B=[112] shows streaking similar to that for 2090 and 049(0), indicating that 049(1.3) is strengthened by one of the platelike precipitates with a {111} habit plane, i.e., either T_1 or Ω. The δ'-phase reflections are <u>not</u> present for this alloy. The SAD pattern with B=[112] for alloy 049(1.9) (Fig. 3b) shows δ' reflections and streaking, indicating that both δ' and T_1-type precipitates are present.

A comparison of the SAD patterns for 049(1.3) and 049(1.9) with B=[110] confirms the presence of δ' in 049(1.9) (Fig. 4). Streaking in the <100> direction, due to precipitation on the {100}, is observed in the SAD pattern for 049(1.9) (Fig. 4c), but not in 049(1.3) (Fig. 4a). A dark-field image (DF) from alloy 049(1.3) with g=[100] and B close to [110] (Fig. 4b) shows only the very faint outline of T_1-type platelets probably due to streaking from a higher order Laue zone. The DF image for alloy 049(1.9) under similar

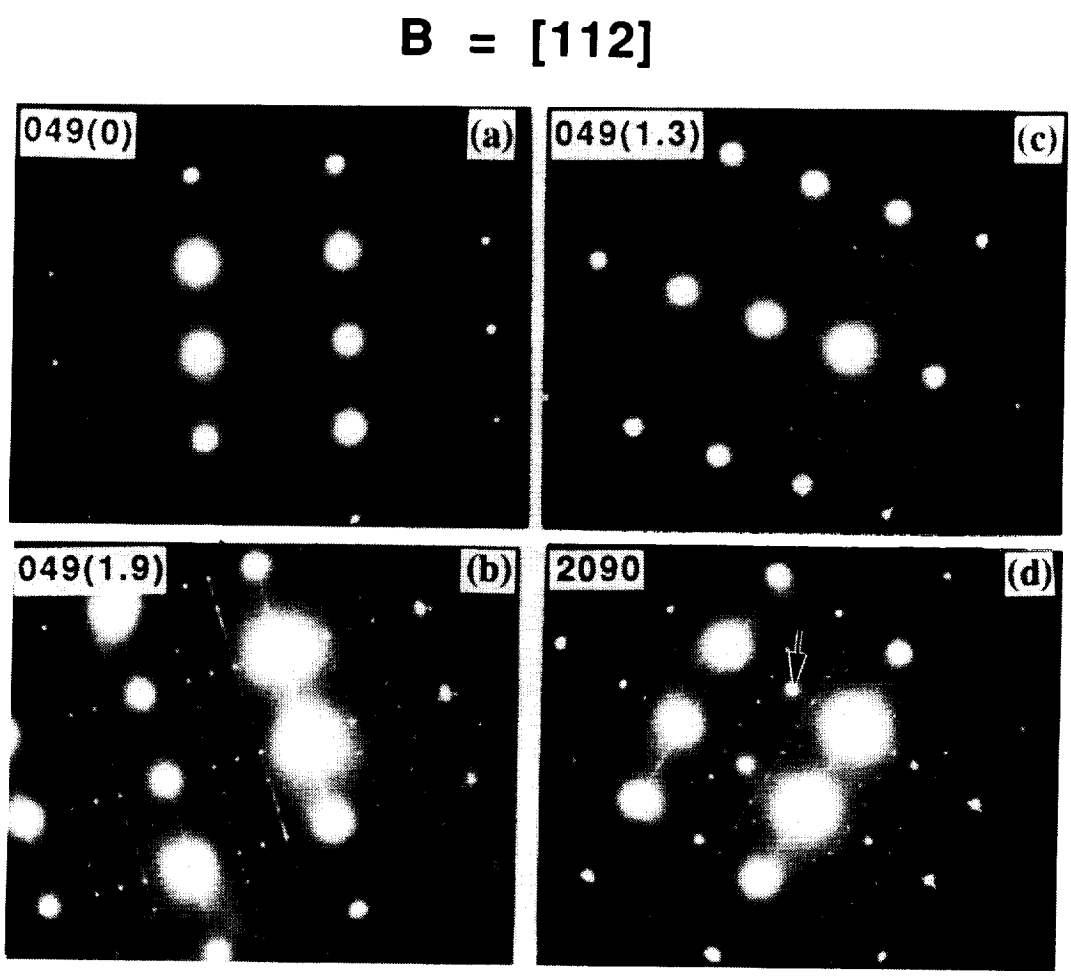

Figure 3. SAD patterns with B=[112] for (a) 2090, (b) 049(0), (c) 049(1.3), and (d) 049(1.9) in the T8 temper.

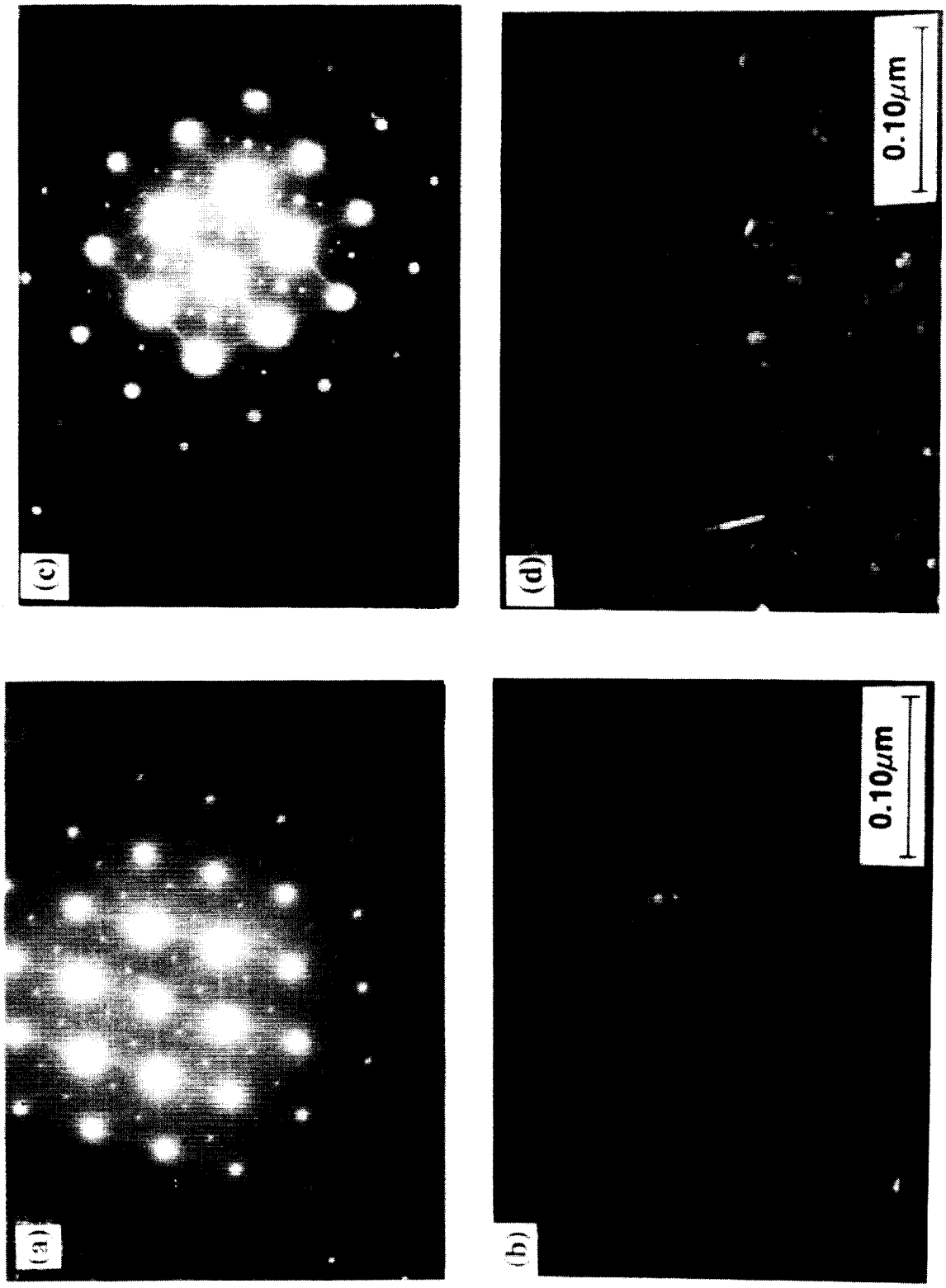

Figure 4. SAD patterns with B=[110] for (a) 049(1.3) and (c) 049(1.9); DF images with g=[100] for (b) 049(1.3) and (d) 049(1.9).

diffraction conditions shows the δ' and β' (Al_3Zr/Al_3Li composite) precipitates and a θ*-type precipitate (Fig. 4d).

Dark-field micrographs for alloys 049(1.3) and 049(1.9), with g=[2020] and B close to the [110] and [111] zone axis, show that the precipitates are regularly shaped (Fig. 5). Huang and Ardell (5) give details of the spatial relationships between the inclined T_1 platelets for alloy 2090, and these relationships should remain unchanged for the platelets in the Weldalite™ 049 alloy regardless of whether they are Ω or T_1. Although neither the volume nor number fraction can be assessed from this limited number of micrographs, qualitatively, the T_1 size and morphology appear similar for the two Weldalite™ alloys.

Based on preliminary HRTEM for T_1-type precipitates in peak-aged 049(1.3), the precipitates are ~10 Å thick and have a stacking sequence similar to that of the T_1 precipitates imaged by Cassada et al. (13) (Fig. 6; note insert). Growth ledges are observed, but, based on the proposed stacking sequence for T_1, all precipitates imaged are essentially one unit cell thick.

DISCUSSION

We propose that the sharp decrease in strength associated with increasing lithium content from 1.3 to 1.9 wt% is associated with the precipitation of δ' at the expense of T_1. A qualitative comparison of the T_1 precipitates in 049(1.3) and 049(1.9) (Fig. 5) indicates that the precipitation of the δ'-phase in 049(1.9) does not change the T_1 precipitate size. Consequently, the variation in strength between 049(1.3) and 049(1.9) is not related to a change in the T_1 platelet size.

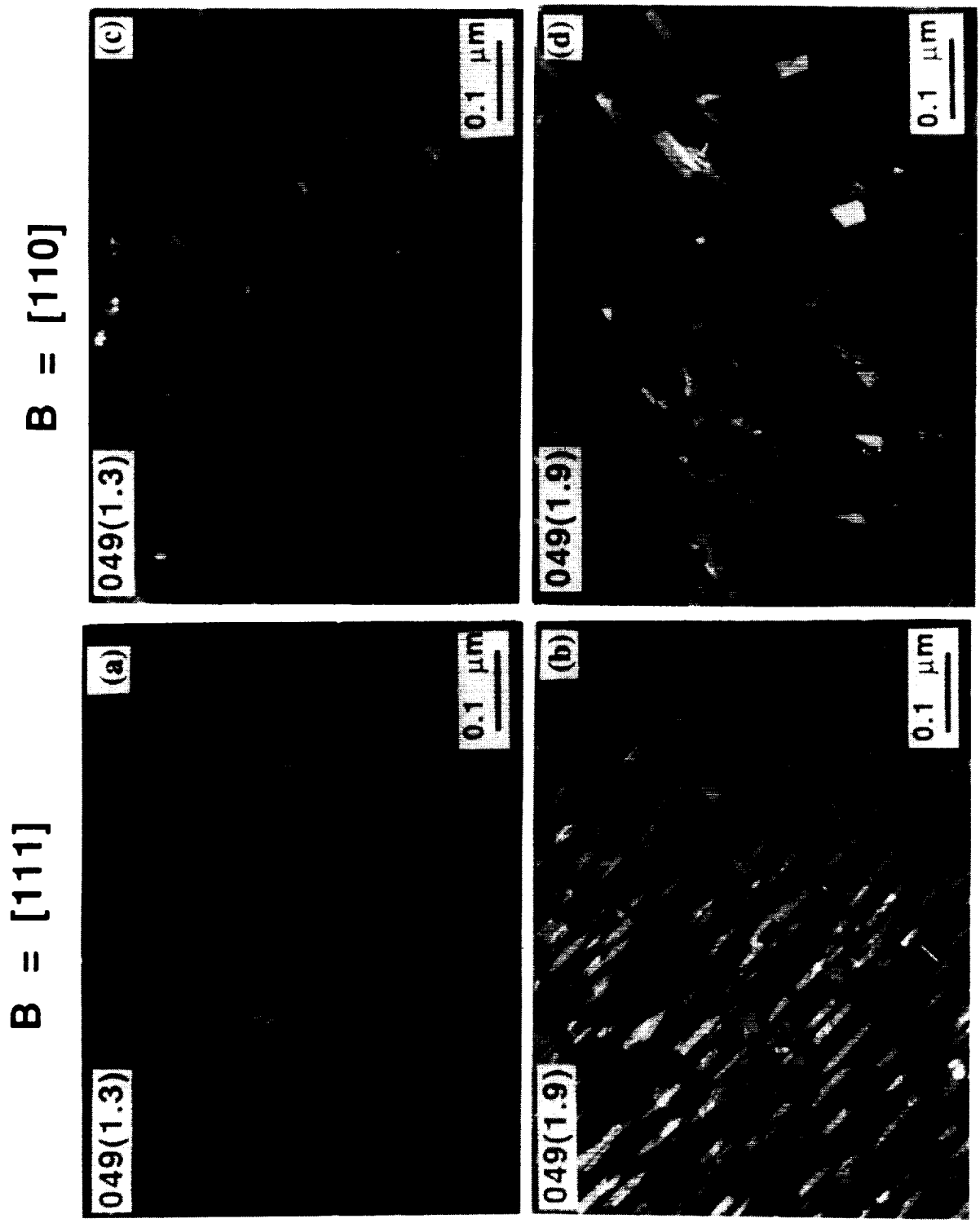

Figure 5. DF images for (a) 049(1.3) and (b) 049(1.9) with g=[2020], B=[110]; for (c) 049(1.3) and (d) 049(1.9) with g=[2020], B=[111].

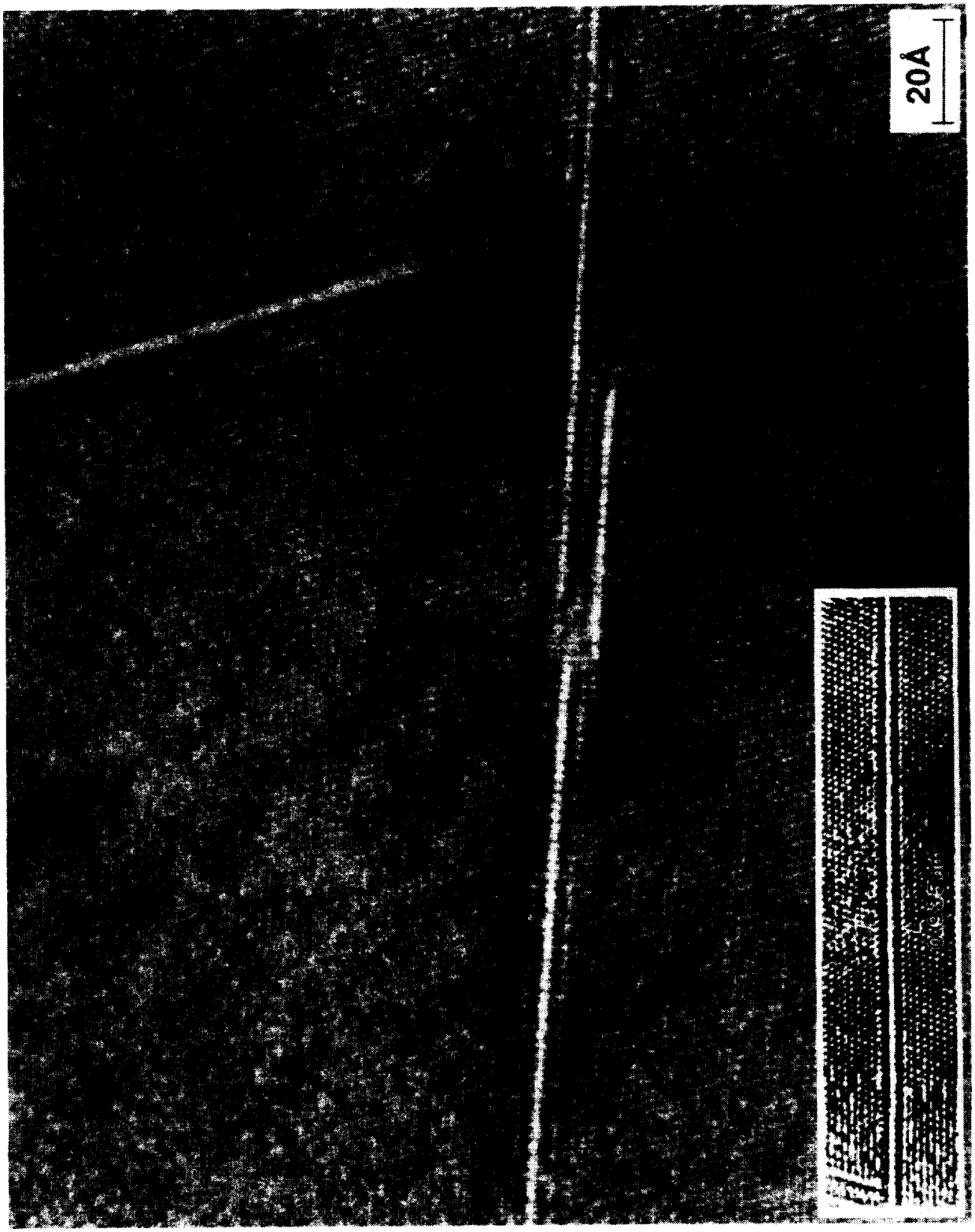

Figure 6. HRTEM for 049(1.3) with B=[111]; insert from Ref. 13.

Huang and Ardell (10,11,14) showed that the T_1-phase is a more potent strengthener than the δ'-phase in Al-Cu-Li alloys, and that the strength contribution from the T_1-phase ($\Delta\tau_{T_1}$) and δ'-phase ($\Delta\tau_{\delta'}$) to the critically resolved shear stress (CRSS) ($\Delta\tau_\rho$) of an alloy follows a generalized superposition rule:

$$\Delta\tau_\rho{}^q = \Delta\tau_{T_1}{}^q + \Delta\tau_{\delta'}{}^q \qquad (1)$$

where q is between 1 and 2.

Thus, if the T_1 distribution and size were to remain constant in the peak-aged temper for alloys 049(1.3) and 049(1.9), then the addition of the δ'-phase would increase strength. The precipitation of δ' in the Weldalite™ 049 variants resulted in a strength decrease, so if this superposition rule is obeyed and solid-solution strengthening effects are small, then the precipitation of δ' would occur at the expense of the T_1-phase. Although we need to obtain supporting quantitative data, based on these assumptions, it appears that precipitation of the δ'-phase must result in a decrease in volume fraction of the T_1-phase.

No θ*-type precipitates were present in 049(0) or 049(1.3), which is contrary to the results of Silcock (3) for ternary alloys with similar compositions. Both alloys have a uniform distribution of very thin, coherent, platelike precipitates with a {111} habit plane. The T_1-phase in 2090 and the Ω-phase in Al-Cu-Mg-Ag alloys are both hexagonal (9) and have platelike morphology with a {111} habit plane. Kerry and Scott (9) determined lattice parameters of a=0.496 nm and c/a=1.414 for the Ω-phase, which are similar to the cell dimensions for T_1 (Al_2CuLi) found by Hardy and Silcock (2), i.e.,

a=0.496 nm and c=0.935 nm (c/a=1.885). Although the stoichiometry of the Ω-phase is unknown, it is believed to be an Al_2Cu-type precipitate. Both Ω and T_1 precipitates have the same crystallographic relationship with the matrix -- $(111)_{Al} \| (0001)_{precipitate}$ -- and a c-axis perpendicular to the face of the platelet. The plate dimensions parallel to the c-axis are very thin. As a result, diffraction from these platelets produces extensive streaking in the reciprocal lattice, which obscures the structure. This streaking, in combination with the identical lengths of the unit cell dimension "a," make it extremely difficult to differentiate T_1 from Ω in the peak-aged temper. Detailed HRTEM is under way to determine if Weldalite™ 049 is strengthened by T_1, Ω, or both phases in the peak-aged temper.

Polmear and coworkers (6-8) and Kerry and Scott (9), showed that Mg and Ag additions stimulate precipitation on the {111} in Al-Cu alloys. Scott et al. (6) proposed that precipitation is stimulated by changing the vacancy-solute interactions and the alloys' stacking fault energy (15). It is also possible that similar mechanisms apply in Weldalite™ 049.

CONCLUSIONS

1. Relatively small amounts of Ag and Mg are extremely effective in stimulating precipitation in Al-6.3Cu-1.3Li-0.4Ag-0.4Mg-0.14Zr alloy, Weldalite™ 049, resulting in a homogeneous distribution of fine, platelike precipitates with a {111} habit plane in the peak-aged, T8 temper.

2. The yield and tensile strengths are strongly dependent on Li content, with a peak in the range of 1.1 to 1.4 wt% Li. At >1.4 wt% Li, strength decreases rapidly, which is associated with δ' precipitation.

3. From HRTEM, the structure of T_1-type precipitates in Weldalite™ 049 is similar to that of T_1 platelets in 2090.

ACKNOWLEDGEMENTS

This work was supported by NASA Contract #NASI-18531, and the authors wish to thank Bill Brewer, Contract Monitor, for his support. We are especially grateful to Dr. F.H. Heubaum for generating some of the mechanical property data on the Weldalite™ alloys. We would also like to thank Drs. F.H. Heubaum, F.W. Gayle, and A.J. Ardell for their enlightening discussions.

REFERENCES

(1) Pickens, J.R., Heubaum, F.H., Langan, T.J., and Kramer, L.S., Proc. of Fifth Int. Conf. on Al-Li Alloys, Williamsburg, Virginia, 1989.

(2) Hardy, H.K. and Silcock, J.M., J. Inst. Metals, Vol. 84, 1955-56, pp. 423-428.

(3) Silcock, J.M., J. Inst. Metals, Vol. 88, 1959-60, pp. 357-364.

(4) Rioja, R.J. and Ludwiczak, E.A., "Aluminum-Lithium Alloys III," Edited by C. Baker et al., Inst. of Metals, London, 1986, pp. 471-482.

(5) Huang, J.C. and Ardell, A.J., Mat. Sci. and Tech., Vol. 3, 1987, pp. 176-188.

(6) Chester, R.J. and Polmear, I.J., "The Metallurgy of Light Alloys," Inst. of Metallurgists, London, 1983, pp. 75-81.

(7) Polmear, I.J. and Couper, M.J., Met. Trans., Vol. 19A, 1988, pp. 1027-1035.

(8) Vietz, J.T. and Polmear, I.J., J. Inst. Metals, Vol. 94, 1966, pp. 410-419.

(9) Kerry, S. and Scott, V.D., Met. Sci., Vol. 18, 1984, pp. 289-294.

(10) Huang, J.C. and Ardell, A.J., Acta Met., Vol. 36, 1988, pp. 2995-3006.

(11) Huang, J.C. and Ardell, A.J., "4th International Aluminum-Lithium Conf.," Edited by G. Champier et al., pp. C3-373-396; J. Phys., 48, Collegue C3, Suppl. 9, Les Editions de Physique, Les Ulis, France, 1987.

(12) J.R. Pickens, F.H. Heubaum, L.S. Kramer, and K.S. Kumar, U.S. Patent Application Serial No. 07/327,927 Filed March 23, 1989 which is a Continuation-in-Part (CIP) of Serial No. 083,333 Filed August 10, 1987.

(13) Cassada, W.A., Shiflet, G.J., and Starke, E.A., ibid. Ref. 11, pp. C3-397-406.

(14) Huang, J.C. and Ardell, A.J., "Aluminium Technology '86," Edited by T. Sheppard, Inst. of Metals, London, 1986, pp. 434-441.

(15) Scott, V.D., Kerry, S., and Trumper, R.L., Met. Sci. and Tech., Vol. 3, 1987, pp. 827-834.

II. THE INFLUENCE OF Ag+Mg ADDITIONS ON THE NUCLEATION OF STRENGTHENING PRECIPITATES IN A NON-COLD-WORKED Al-Cu-Li ALLOY

THE INFLUENCE OF Ag+Mg ADDITIONS ON THE NUCLEATION OF STRENGTHENING PRECIPITATES IN A NON-COLD-WORKED Al-Cu-Li ALLOY

Introduction

Aluminum-copper-lithium alloys generally require cold work to attain their highest strengths in artificially aged tempers (1,2). These alloys are usually strengthened by a combination of the metastable $\delta'(Al_3Li)$ and $\theta'(Al_2Cu)$ phases and the equilibrium T_1 (Al_2CuLi) phase (3), where the T_1 phase is a more potent strengthener than the δ' (4). Various investigators, such as Cassada et al. (5) and Lee and Frazier (6), have shown that the high strengths obtained after artificial aging associated with cold work result from the heterogeneous precipitation of T_1 on matrix dislocations.

Pickens and coworkers (7-9) have shown that the Al-(4-6.3)Cu-1.3Li-0.4Ag-0.4Mg-0.14Zr (wt%) alloy Weldalite™ 049 attains ultra-high strengths in artificially aged tempers both with and without prior cold work (i.e., the T8 and T6 tempers, respectively). The T8 temper is primarily strengthened by a uniform distribution of fine T_1-type* platelike precipitates with a {111} habit plane (8), whose nucleation is stimulated by the Ag+Mg additions (7,8). These precipitates are also observed in the T6 temper. Moreover, Gayle et al. (10,11) identified numerous strengthening phases in non-cold-worked, artificially aged conditions, with the T_1 phase being predominant at peak strength. The resulting ultra-high strength in the T6 temper (i.e., without cold work) gives Weldalite™ 049 many potential advantages over other

* The strengthening phase is referred to as T_1-type because of difficulties in unambiguously indexing it as the T_1-phase or Ω-phase due to the similarities in the electron diffraction patterns from the two phases (8).

Al-Cu-Li alloys. The objective of the work reported here is to elucidate the mechanism by which the Ag+Mg additions stimulate the precipitation of T_1-type precipitates without cold work. To accomplish this, the microstructure of an Al-6.3Cu-1.3Li-0.14Zr model alloy was evaluated in a T6-type temper with and without the Ag+Mg addition.

Materials and Experimental Procedure

Two billets weighing 23 kg each were cast at Martin Marietta Laboratories and extruded into 0.95 x 10.2-cm bars at a ratio of 20:1 at International Light Metals, Torrance, CA. After extrusion, the bars were solution-heat-treated (SHT) at 504°C and water-quenched to ambient temperature. Compositions were measured from the extruded bar using the inductively coupled plasma technique (Table 1).

TABLE 1

Alloy Compositions

		Cu	Li	Zr	Ag	Mg	Al
049 [0Ag+0Mg]	nominal wt%	6.30	1.30	0.14	--	--	bal
	measured wt%	5.83	1.25	0.14	0	0	bal
	at%	2.48	4.85	0.04	--	--	bal
049	nominal wt%	6.30	1.30	0.14	0.40	0.40	bal
	measured wt%	6.47	1.25	0.14	0.40	0.40	bal
	at%	2.77	4.88	0.04	0.10	0.43	bal

The alloys will be referred to as 049 and 049 [0Ag+0Mg] as shown. Specimens were artificially aged and examined by transmission electron microscopy (TEM) with a JEOL 100CX. TEM foils were prepared with a Struers Tenupol using an electrolyte of one part HNO_3 in three parts methanol.

Results

Both alloys were evaluated by TEM after aging for 24 h at 180°C. This temper was chosen based on the tensile strength aging curve for alloy 049. The ultimate tensile strength (UTS), yield strength (YS), and percent elongation (%el) for the alloys in this temper were: 675 MPa YS, 707 MPa UTS, and 3.7% el for alloy 049, and 345 MPa YS, 478 MPa UTS, and 8.3% el for alloy 049 [0Ag+0Mg].

The selected-area electron diffraction pattern (SADP) for 049[0Ag+0Mg] with B = [100] (Fig. 1a) shows streaking in the <100> directions, with more intense streaks in one direction than the other. The <100> streaking is also present on the SADP with B = [110] (Fig. 1b). These <100> streaks result from θ' precipitates (12) and have maximum at the aluminum spots and at the superlattice positions. No other streaking or reflections is present on SADPs for either zone axis.

Faint but continuous streaking in the <111> direction is present on the SADP from 049 [0Ag+0Mg] with B = [112] (Fig. 1c). Two sets of reflections are present, one at 1/2 {220}, 1/3 {220}, and 2/3 {220}, and another at 1/3 and 2/3 {042}. Satellite (at arrow in Fig. 1c) spots along the <042> direction appear to be related to these reflections. Similar <111> streaking and

049 [0Ag + 0Mg] T6

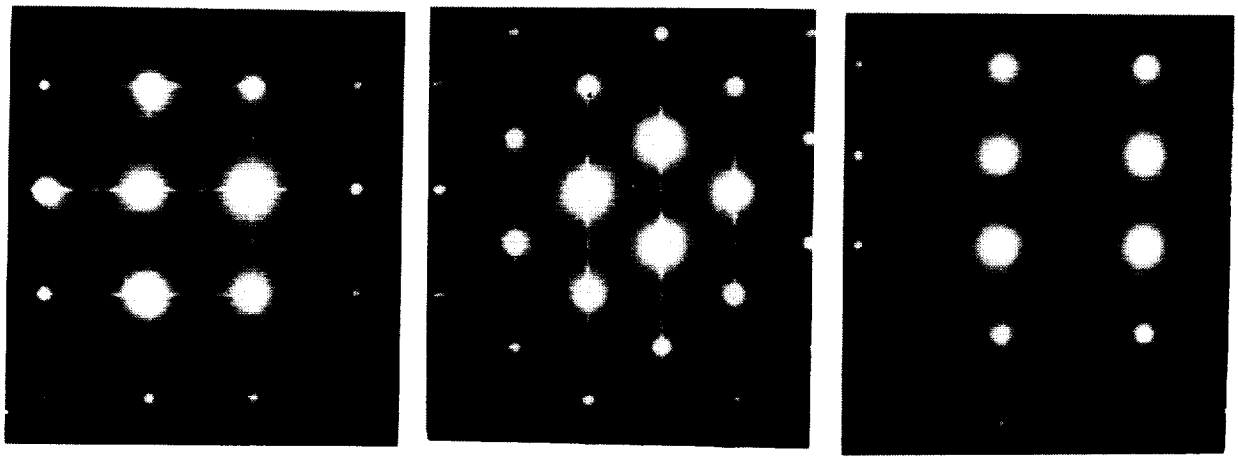

FIG. 1 SADPs for alloy 049 [0Ag+0Mg] T6 with (a) B = [100], (b) B = [110], and (c) B = [112].

reflections at 1/3 and 2/3 {220} were indexed as the T_1 phase in alloy 2090 by Huang and Ardell (4).

The SADP for 049 with B = [100] (Fig. 2a) shows reflections centered at 1/3 {220} and 2/3 {220}, which result from the intersection of two streaks in reciprocal space. Thus, when the deviation parameter ($\bar{s}$) is equal to zero, these reflections are single spots. When $\bar{s}$ does not equal zero, two satellite spots are present, separated by a distance that varies with $\bar{s}$. Similar reflections at 1/3 {220} and 2/3 {220} are also present on the SADP with B = [110] (Fig. 2b), accompanied by streaks in the <111> directions with diffuse maxima at approximately 1/2 {111}. No <100> streaking is present on the SADPs with B = [110] or [100]. Sharp <111> streaking with maxima at 1/4, 1/2, and 3/4 {111} is also present on the SADP with B = [112] (Fig. 2c). Elongated reflections are present at 1/3 {131}, 2/3 {131}, 1/3 {042}, and 2/3 {042}. These reflections, and the <111> streaking, result from T_1-type precipitates on {111} planes. The superlattice reflections at 1/2 {220} probably result from Al_3Zr.

A brightfield (BF) micrograph of 049[0Ag+0Mg] (Fig. 3a) shows θ' precipitates surrounding heterogeneous T_1 platelets. The brightfield was imaged with B = [110] so that one set of θ' precipitates is oriented normal to the plane of the foil and, thus, is viewed nearly edge on. The darkfield (DF) micrograph, which was imaged using the superlattice maxima on the <100> streak, shows a θ' precipitate-free zone (PFZ) surrounding the T_1 platelets (Fig. 3b). A θ' PFZ is also present next to the grain boundary (GB) in the upper right-hand corner of the micrograph.

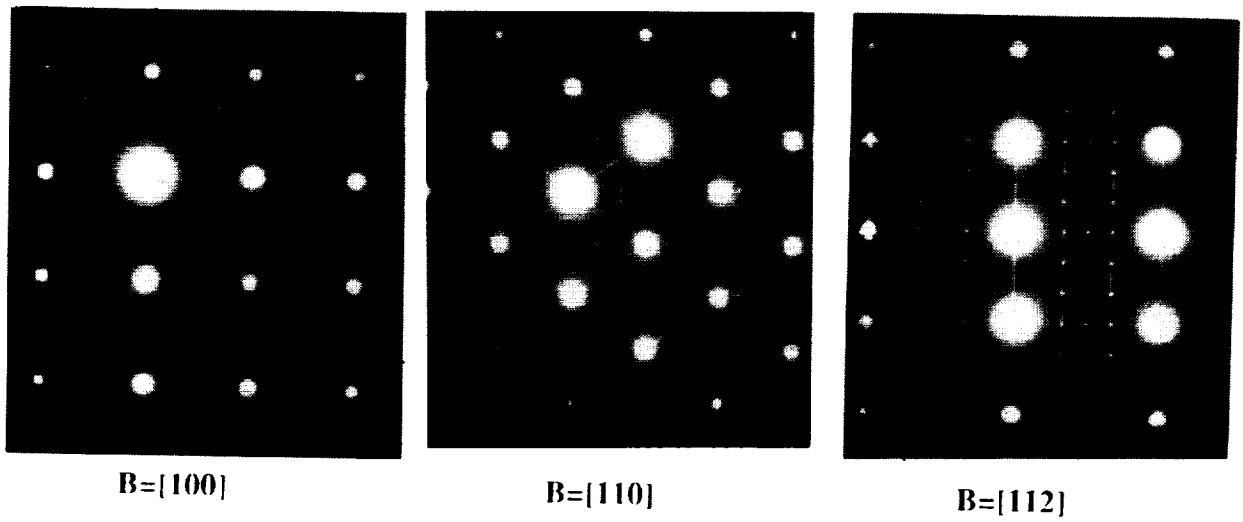

FIG. 2 SADPs for alloy 049 T6 with (a) B = [100], (b) B = [110], and (c) B = [112].

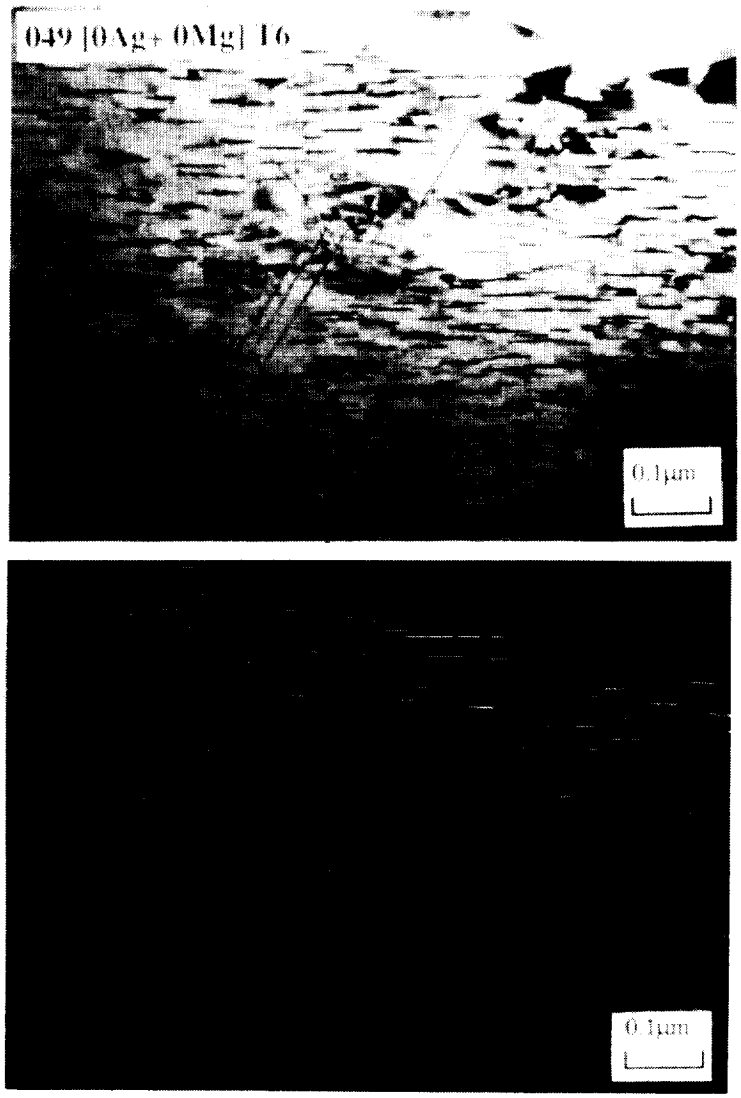

FIG. 3 (a) Brightfield micrograph for 049 [0Ag+0Mg] T6 (B = [110]), and (b) dark-field micrograph, g = [100].

The BF micrograph for 049 (also imaged with B = [110]) shows a fairly uniform distribution of T_1-type precipitates (Fig.4a) that are about 10Å in thickness and appear to have about the same diameter as the heterogeneous T_1 precipitates in 049[0Ag+0Mg] (Fig. 3a). In this orientation, two T_1 variants are normal to the plane of the foil and two are inclined at about 35° (12). The DF micrograph (Fig. 4b) shows the T_1-type precipitates that are nearly normal to B.

Comparing the T6 microstructures of 049[0Ag+0Mg] and 049 shows that the distribution of the strengthening phases is strongly influenced by the Ag+Mg addition (Table 2).

Table 2

Strengthening Phases After 24 h Aging at 180°C

(based on electron diffraction results)

Alloy	Phases/Diffraction Results	Relative Distribution
049[0Ag+0Mg]	T_1 (Al_2CuLi)	Nonhomogeneous with θ' PFZ
	θ'(Al_2Cu)	Nonhomogeneous; predominant strengthening phase
	α'(Al_3Zr/Al_3Li)	Minor
049	T_1-type; T_1(Al_2CuLi) and/or Ω (Al-Cu)	Homogeneous
	θ'	None
	Al_3Zr	Minor

As shown in Figs. 3b and 5a, a θ' PFZ exists along the GB for 049[0Ag+0Mg]. T_1 precipitates cross the θ' PFZ in 049 [0Ag+0Mg] (Fig. 5 at the arrow) and are present right up to the boundary in 049 (Fig. 5b).

FIG. 4 (a) Brightfield mimcrograph for 049 T6 (B = [110]) and (b) dark-field micrograph using center of ⟨111⟩ streak.

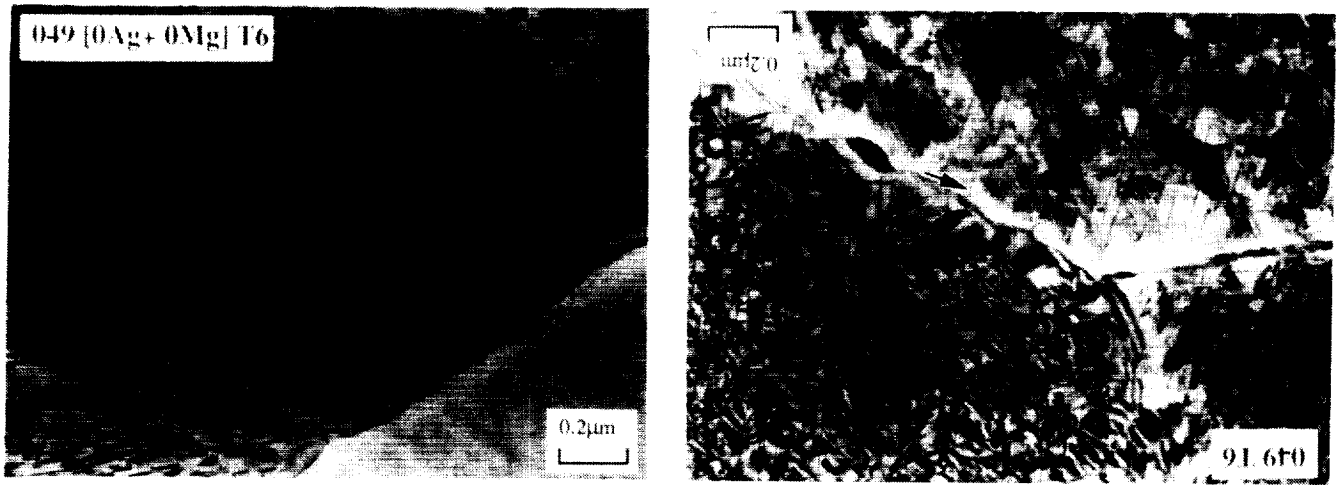

FIG. 5 Brightfield micrographs of high-angle grain boundaries (B = [110]) in (a) 049[0Ag+0Mg] T6 and (b) 049 T6.

Discussion

The distribution of strengthening phases in the Al-6.3Cu-1.3Li-0.14Zr (wt%) alloy with a Cu/Li wt% ratio of 4.8 is substantially altered by small additions of Ag+Mg. As shown in Fig. 3, θ' and heterogeneous T_1 are the primary strengthening phases in alloy 049[0Ag + 0Mg] artificially aged to a near-peak strength without cold work. Silcock (13) observed the same phase assemblage after artificially aging Al-Cu-Li ternary alloys with similar compositions for 16 h at 165°C. The addition of Ag+Mg (i.e., alloy 049) results in a uniform distribution of fine T_1-type precipitates (Fig. 4). Recent work by Gayle et al. (11) showed that θ', S'(Al_2CuMg), and a phase designated as ν could also be present in the matrix of Weldalite™ 049 in the T6 temper. Although no diffraction was observed from other strengthening precipitates in the present study, it is possible that some may be present at volume fractions that are too low to provide detectable diffraction information on the SADPs. Thus, the Ag+Mg addition results in an increase in the stability of T_1-type precipitates, apparently at the expense of the θ' phase.

Nucleation of T_1 in an Al-2.4Li-2.4Cu-0.18Zr alloy was shown by Cassada et al. (5) to require the presence of Shockley partial dislocations. They (5) proposed that most of the Shockley partials result from cold work after quenching, which is consistent with the finer T_1 distribution and increased strengthening that accompanies increased cold work. In the present study, alloy 049 without prior cold work displays a uniform distribution of fine T_1-type precipitates. Therefore, the addition of Ag+Mg must either significantly

increase the number of Shockley partial dislocations -- unlikely for a non-cold-worked temper -- or enhance the nucleation of T_1-type precipitates by some other mechanism. Perhaps the Ag+Mg increases the number fraction of collapsed vancancy loops (i.e., Frank partial dislocations) which then serve as effective sites for nucleation of T_1-type precipitates.

A number of workers (13-21) have investigated the effect of Ag+Mg on precipitation in Al-Cu alloys. Chester and Polmear (14) identified a novel strengthening phase, which they called Ω. Some controversy exists as to the structure of the Ω-phase, with Kerry and Scott (15) assigning it a hexagonal structure, Auld (19) assigning it a monoclinic structure, and Muddle and Polmear (16) and Knowles and Stobbs (20) assigning it an orthorhombic structure. Auld and Vietz (17) proposed that Ω is isostructural with the T_1-phase (Al_2CuLi) observed in Al-Cu-Li alloys. Regardless of the exact structure of the Ω-phase, Scott et al. (19) showed that when Ag+Mg are added to an Al-Cu alloy, the Ω-phase becomes more stable than θ'; as a result, the volume fraction of the θ'-phase decreases and the volume fraction of the Ω-phase increases with increased artificial aging. Since Mg and Ag additions lower the stacking fault energy (SFE) of aluminum (18), Scott et al. (21) hypothesized that the decreased SFE enhanced segregation of solute to the {111} planes, which then acted as nuclei for the Ω-phase (the Ω-phase has a {111} habit plane in the Al-Cu system).

Faulted loops surrounded by Frank partial dislocations ($b=1/3[111]$) form when a vacancy disk collapses. As the size of the loop increases, the stacking fault disappears and a complete loop with $b = 1/2\ [110]$ is nucleated (22). The critical size at which the complete loop nucleates is

related to the SFE: the lower the SFE, the larger the critical size. The Ag+Mg in alloy 049 could affect the formation and stability of these partials in two ways. First, the high affinity between Mg and vacancies (23) will increase the number of vacancies retained in the microstructure after quenching from the SHT temperature and, consequently, increase the number of vacancies available to form loops. Second, the decrease in SFE induced by Ag+Mg might stabilize the Frank partials (23). Also, the stacking fault could be further stabilized by an increase in the solute concentration on the Frank partial dislocation due to the Suzuki effect (24): solute concentration on the stacking fault is different from that in the matrix due to changes in the chemical potential of the solute. These stacking faults with high solute concentration could then act as nucleation sites for T_1-type precipitates.

In summary, we have shown that the Ag+Mg addition increases the precipitation of T_1-type precipitates on {111} planes in the non-cold worked artificially aged temper and we propose a mechanism whereby an increase in the formation and stability of the Frank partial dislocations provides nuclei for T_1-type precipitates. An investigation is currently under way to determine the Burgers vector of the dislocation at the precipitate-matrix interface.

Acknowledgement

This work was supported by NASA contract #NAS1-18531. The authors wish to thank W. Brewer, contract monitor, for his support. We also wish to thank F.W. Gayle, K.S. Kumar, and J.D. Venables for their enlightening discussions.

References

1. R.F. Ashton, D.S. Thompson, E.A. Starke, Jr., and F.S. Lin, in Al-Li Alloys III, C. Baker, P.J. Gregson, S.J. Harris, and C.J. Peel, eds., Inst. of Metals, London (1986).
2. T.H. Sanders Jr., and E.A. Starke, Jr., in Proc. of the Fifth Int. Al-Li Conf., T.H. Sanders, Jr., and E.A. Starke, Jr., eds., Mater. and Component Eng. Pub. Ltd., London (1989).
3. T.H. Sanders and E.A. Starke, in Aluminum-Lithium Alloys II, T.H. Sanders, Jr., and E.A. Starke, Jr., eds., TMS-AIME, Warrendale, PA, pp. 1-15 (1983).
4. J.C. Huang and A.J. Ardell, Acta Metall., 36, pp. 2995-3006 (1988).
5. W.A. Cassada, G.J. Shiflet, and E.A. Starke, Jr., in 4th Int. Aluminum-Lithium Conf., G. Champier, B. Dubost, D. Miannay, and L. Sabetay, eds., Soc. Francaise de Metallurgie, Paris, France, pp. C3-397-406 (1987); J. de Physique (France), 1987, 48, (9) (1987).
6. E.W. Lee and W.E. Frazier, Scripta Metall., 22, pp. 53-57 (1988).
7. J.R. Pickens, F.H. Heubaum, T.J. Langan, and L.S. Kramer, ibid. Ref. 2, p. 1397.
8. T.J. Langan and J.R. Pickens, ibid. Ref. 2, p. 691.
9. J.R. Pickens, F.H. Heubaum and L.S. Kramer, Scripta Metall. et Mater., 24, pp. 457-462 (1990).
10. F.W. Gayle, F.H. Heubaum, and J.R. Pickens ibid. ref. 2, pp. 701-710.
11. F.W. Gayle, F.H. Heubaum, and J.R. Pickens, Scripta Metall., 24, pp. 79-84 (1990).

12. A. Kelly and R.B. Nicholson, Prog. Metall. Sci., 10 (3), p. 193 (1963).

13. J.M. Silcock, J. Inst. Metall., 88, pp. 357-364 (1959-60).

14. R.J. Chester and I.J. Polmear, in The Metallurgy of Light Metals, Inst. of Metallurgists, London, pp. 75-81 (1983).

15. S. Kerry and V.D. Scott, Metall. Sci., 18, pp. 289-294 (1984).

16. B.C. Muddle and I.J. Polmear, Acta Metall., 37 (3), pp. 777-789 (1989).

17. J.M. Auld and J.T. Vietz, in The Mechanism of Phase Transformations in Crystalline Solids, 77, The Inst. of Metals, London (1969).

18. P.C.J. Gallagher, Metall. Trans., 1, pp. 2429-2461 (1970).

19. J.H. Auld, Mat. Sci and Tech., 2, pp. 784-787 (1986).

20. K.M. Knowles and W.M. Stobbs, Acta Cryst., B44, pp. 207-227 (1988).

21. V.D. Scott, S. Kerry, and R.L. Trumper, Mater. Sci. and Technol., 3, pp. 827-834 (1987).

22. F. Kroupa, in Theory of Crystal Defects, Proc. of the Summer School held in Hrazany, B. Gruber, ed., Academic Press, NY, pp. 275-316 (1964).

23. K.H. Westmacott, R.S. Barnes, D. Hull, and R.E. Smallman, Philos. Mag., 6, pp. 929-935 (1961).

24. H. Suzuki, Sci. Rep. Res. Inst. Tohoku Univ., A-4, p. 452 (1952).

III. THE EFFECT OF TiB_2 REINFORCEMENT ON THE MECHANICAL PROPERTIES OF AN Al-Cu-Li ALLOY-BASED METAL-MATRIX COMPOSITE

THE EFFECT OF TiB_2 REINFORCEMENT ON THE MECHANICAL PROPERTIES OF AN Al-Cu-Li ALLOY-BASED METAL-MATRIX COMPOSITE

Introduction

The addition of ceramic particles to aluminum-based alloys (1,2) can substantially improve mechanical properties, especially Young's Modulus and room- and elevated-temperature strengths. However, these improvements typically occur at the expense of tensile ductility. In the work reported here, we evaluated the mechanical properties of a metal-matrix composite (MMC) consisting of an ultra-high-strength aluminum-lithium alloy, Weldalite™ 049, reinforced with TiB_2 particles produced by an in-situ precipitation technique called the XD™ process. The results were compared to the behavior of a non-reinforced Weldalite™ 049 variant.

Weldalite™ 049 is an Al-(4-6.3)Cu-1.3Li-0.4Mg-0.4Ag-0.14Zr alloy which typically attains tensile strengths in excess of 700 MPa in the near-peak-aged tempers (3). These ultra-high strengths are promoted by the Ag+Mg additions, which increase the nucleation of a T_1-type* platelike strengthening precipitate with a {111} habit plane (4). Due to its unique microstructure, this alloy does not exhibit the relatively low ductility at high strength

* The strengthening phase is referred to as T_1-type because of difficulties in unambiguously indexing it as the T_1-phase or Ω-phase due to similarities in the electron diffraction patterns from the two phases (4).

levels commonly associated with aluminum-lithium alloys. Thus, it is a promising candidate for a MMC matrix material.

Modulus, already enhanced by the presence of lithium in the Weldalite™ 049 alloy (5), should be further increased by the addition of high-modulus (496 GPa) TiB_2 particles. The addition of TiB_2 produced by the XD™ process has been shown to improve strength retention at elevated-temperatures for other aluminum alloys (6). TiB_2 is an attractive reinforcement because it has good wettability with liquid aluminum.

Materials and Experimental Procedures

TiB_2-reinforced and non-reinforced Weldalite™ 049 variants were cast into ~23-kg ingots at Martin Marietta Laboratories under an argon cover. The TiB_2 particles used for the MMC were produced by the XD™ process and added at a nominal volume fraction of 4.0 v% to the molten Weldalite™ 049 alloy just prior to casting. We used this relatively low volume fraction for a preliminary assessment of the feasibility of TiB_2 reinforcement of Weldalite™ 049, with higher TiB_2 loadings to follow contingent on the results of this evaluation. The ingots were homogenized, scalped, and extruded at 370°C into 9.5-mm x 102-mm bar. Following extrusion, both bars were solution-heat-treated (SHT) at 504°C for 1 h, water-quenched to room temperature, and stretched 2.5 and 3.5% for the Weldalite™ 049-TiB_2 and Weldalite™ 049, respectively.** The compositions for the two alloys were determined by the

** Referred to as 049-TiB_2 and 049 hereafter.

inductively coupled plasma technique. The measured composition for 049 in wt% was Al-5.98Cu-1.3Li-0.38Ag-0.40Mg-0.14Zr with less than 0.01 % B or Ti. That of 049-TiB_2 was Al-6.28Cu-1.38Li-0.34Ag-0.42Mg-0.15Zr with 1.65%B and 3.90%Ti.

The variation in tensile properties with aging time at 160°C was measured for both alloys. Room-temperature testing was performed using ASTM standard E-8 subsize flat bar specimens. Tensile testing at elevated, room, and cryogenic temperatures was performed using 6.4-mm-diameter round tensile specimens. Tensile properties were measured at elevated temperature after 0.5-h or 100-h exposures, and at room temperature after a 100-h exposure at elevated temperature. Specimens exposed for 100 h and tested at temperature were held for 99.5 h at temperature in air, furnace cooled, reheated to the test temperature in the Instron test apparatus, and held at temperature for 0.5 h prior to testing. Specimens exposed for 0.5 h and tested at temperature were held for that time in the furnace on the Instron and tested. Temperature was monitored by a thermocouple placed in contact with the grip section of the specimen.

Dynamic modulus was determined for both alloys by ultrasonic measurements in the three orthogonal principal directions on 0.95-cm cubes cut from the extruded bar in the T3 and T8 tempers. Transmission electron microscopy (TEM) was used to identify strengthening precipitates in the peak-aged (T8) temper.

Results

Optical microstructural evaluation of the 049-TiB_2 alloy showed that the TiB_2 particles were approximately ~ 1 μm in diameter and were evenly distributed throughout the matrix, with the exception of those "tied up" in large agglomerated clusters (Fig. 1). Although there may have been some interaction between the primary-phase particles* in the matrix and the TiB_2 particles, it is clear that these clusters resulted from the XD™ process and were not related to the aluminum-lithium alloy matrix. The total volume fraction of TiB_2 was between 3.2 and 3.7%, based on chemcial analysis and the assumption that all the B was tied up as TiB_2. Because both alloys were extruded into flat bar with a relatively high aspect ratio (10:1), the grains had a pancake morphology with their long axis parallel to the extrusion direction. The grain size was roughly the same for both alloys.

Tensile properties were determined for 049 and 049-TiB_2 after various aging times at 160°C. Both alloys showed a very strong natural aging response, with ultimate tensile strengths (UTS) in the T3 temper (natural aging for 1 yr) of 520 MPa for 049 and 529 MPa for 049-TiB_2. Both alloys underwent a reversion in strength during the initial stages of artificial aging from the T3 temper (Fig. 2), but the aging response was slightly faster for the TiB_2-reinforced variant: peak strength occurred around 10 h for the 049-TiB_2 alloy compared, with 24 h or longer for the 049 alloy. The strength-

* These particles are θ-phase (Al_2Cu) and possibly T_B-phase ($Al_{7.5}Cu_4Li$) precipitates which form during solidification from the melt and do not dissolve during solutionizing.

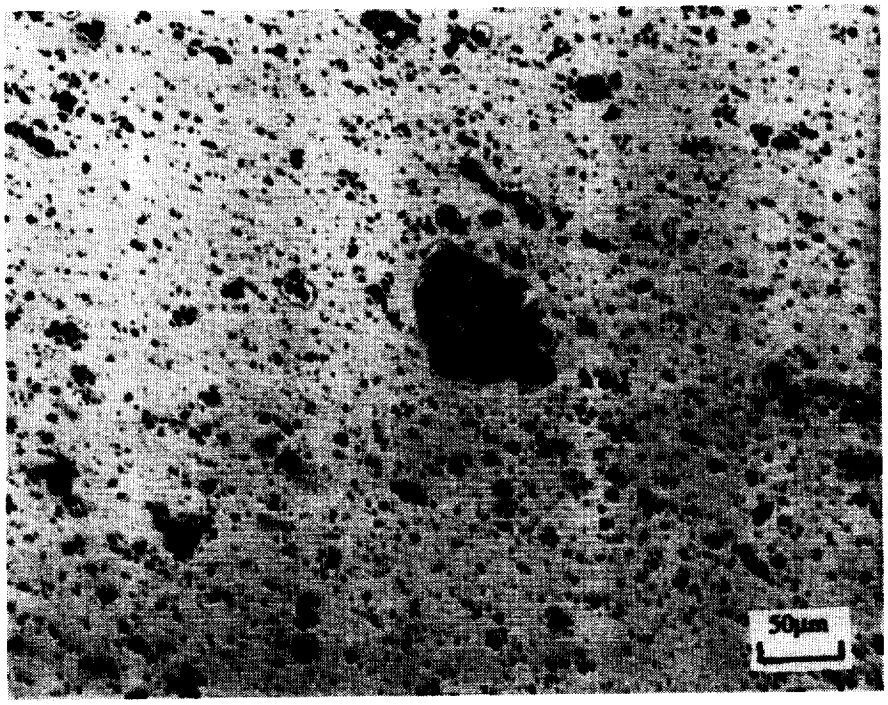

FIG. 1. Optical micrograph showing agglomerated cluster of TiB_2 particles.

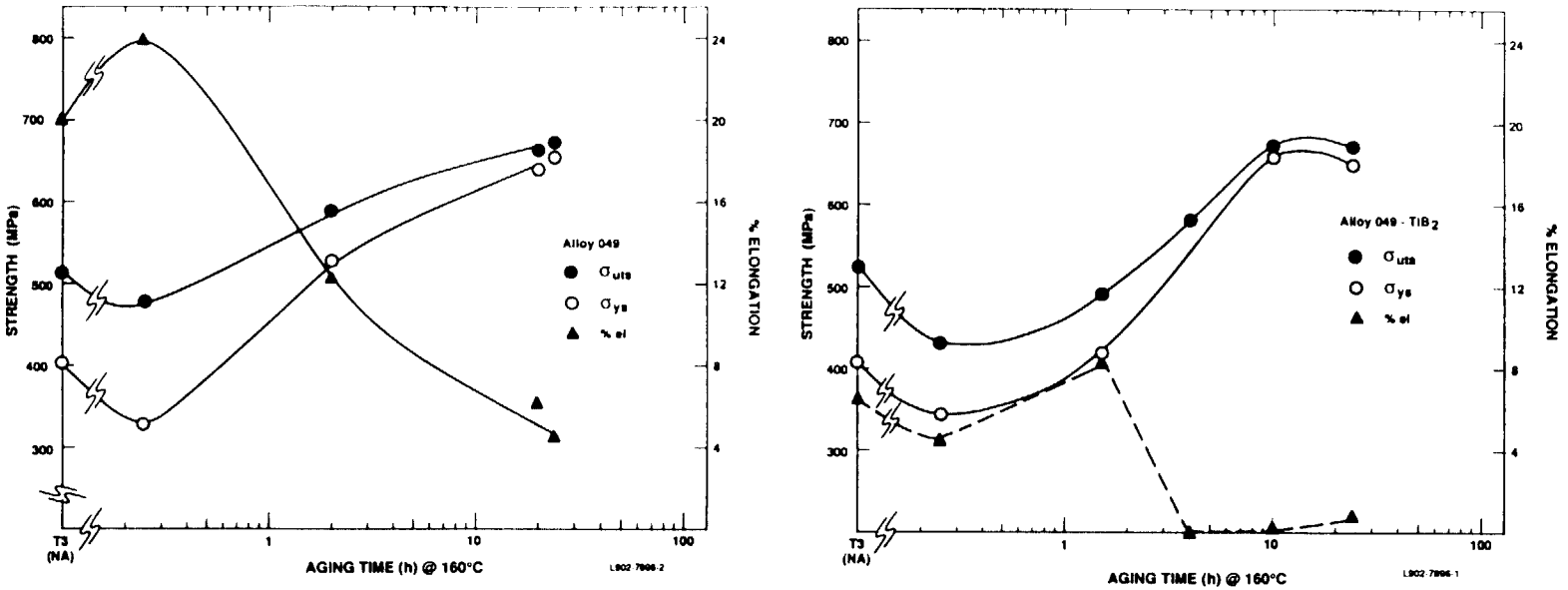

(a) (b)

FIG. 2. Tensile aging curves at 160°C for (a) 049, and (b) 049-TiB_2.

at-peak hardness was virtually the same for both alloys. As would be expected, the large agglomerated clusters drastically reduced the ductility of the 049-TiB_2 alloy (e.g., only 0.9% elongation at the 673-MPa tensile strength level). The ductility of 049 increased dramatically during reversion to 24%, while still maintaining a tensile strength level of 490 MPa. Although the ductility of the 049-TiB_2 matrix may have increased during reversion, the effect was masked in the MMC by fracture initiated at the TiB_2 agglomerates. Selected area electron diffraction (SADP) results showed that after aging for 24 h at 160°C, both alloys were primarily strengthened by T_1-type precipitates (Fig. 3).

Tensile properties were measured for 049 and 049-TiB_2 at temperatures over the range of -194°C to 315°C after 0.5 h or 100 h at temperature (Fig. 4). The tensile strength of 049 increased from 695 MPa at room temperature to 834 MPa at -194°C; 049-TiB_2 showed no increase in tensile strength due to a complete loss of ductility at this temperature. Very little change in strength was observed for either alloy after 0.5 h at temperatures from 23°C to 149°C. Above 149°C, strength decreased with temperature at about the same rate for 049 and 049-TiB_2. The decrease in strength with increasing temperature was steeper when the exposure time was increased to 100 h. Also, the TiB_2-reinforced alloy showed a slightly greater decrease in strength than the non-reinforced variant over this region. Nevertheless, the strength of each alloy at temperature decreased only slightly after 100 h at 149°C.

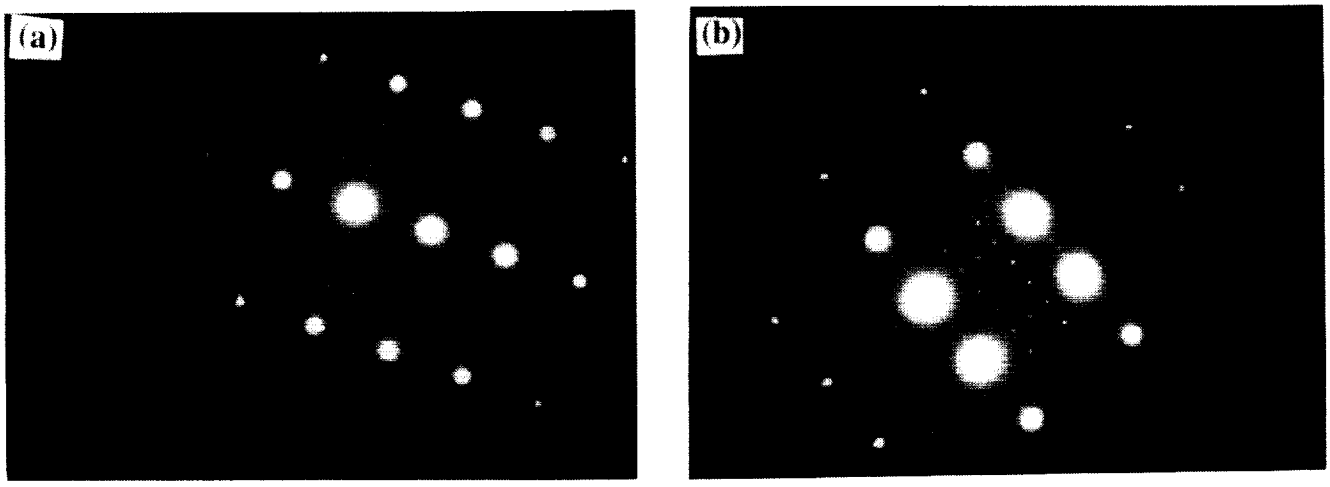

FIG. 3. SADP for (a) 049 and (b) 049-TiB_2.

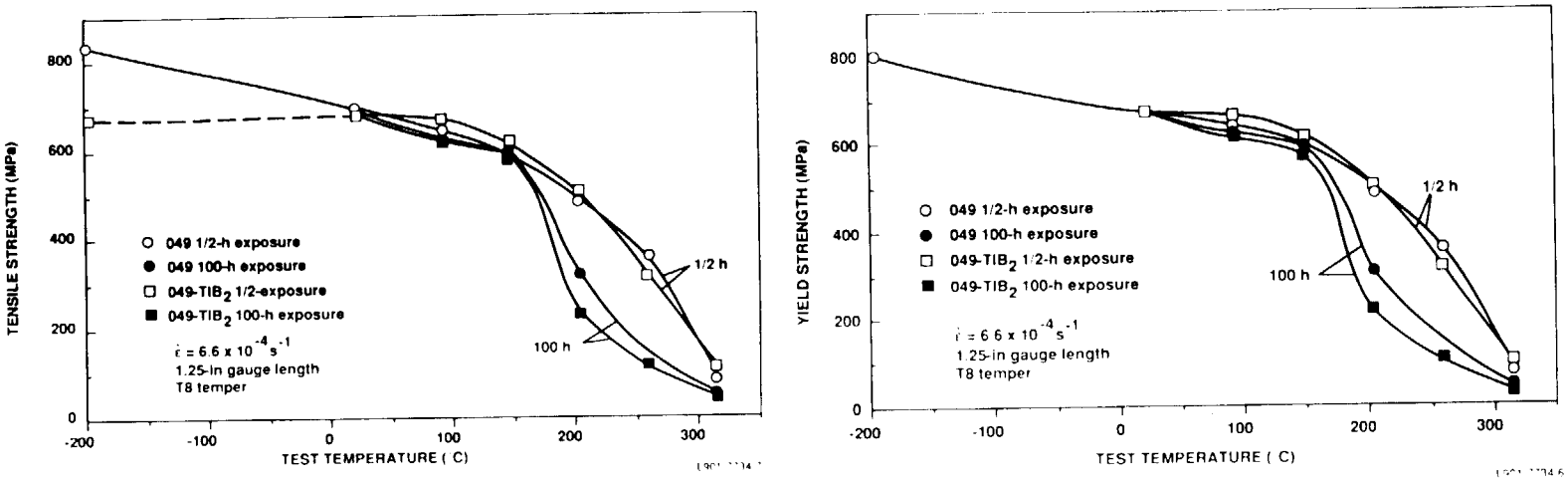

(a) (b)

FIG. 4. Strength at temperature vs. test temperature for 049 and 049-TiB_2 after 0.5 h or 100 h at temperature: (a) ultimate tensile strength, and (b) tensile yield strength.

The alloys were also tested at room temperature after a 100-h exposure to temperatures ranging from 93 to 315°C (Fig. 5). The results of this testing can be categorized by temperature region, with both 049 and 049-TiB_2 showing essentially the same behavior. Exposures from ambient temperature up to 149°C produced no change in either UTS or yield strength (YS). Room-temperature strength fell rapidly with exposures between 149°C and 260°C, and plateaued with little change between 260°C and 316°C. The TiB_2 reinforcement did not increase the elevated-temperature stability of Weldalite™ 049.

Modulus was measured by an ultrasonic technique in the T3 and T8 tempers in the short-transverse (ST), long-transverse (LT), and longitudinal (L) directions from each extruded bar to assess stiffness anisotropies due to texture (Table 1). No effect of orientation was observed in the reinforced variant, while the non-reinforced variant showed a slightly higher modulus in the ST direction for both tempers. TiB_2 reinforcement resulted in about an 8% increase in modulus in both tempers compared with the non-reinforced variant.

Table 1

Ultrasonic Modulus for 049 and 049-TiB_2

Alloy	Temper	Modulus (GPa) ST-Direction	LT-Direction	L-Direction
049	T3	78.3	77.4	77.3
049 TiB_2	T3	84.7	85.3	84.5
049	24 h @160°C	78.9	77.6	77.8
049 TiB_2	24 h @160°C	85.0	85.4	84.7

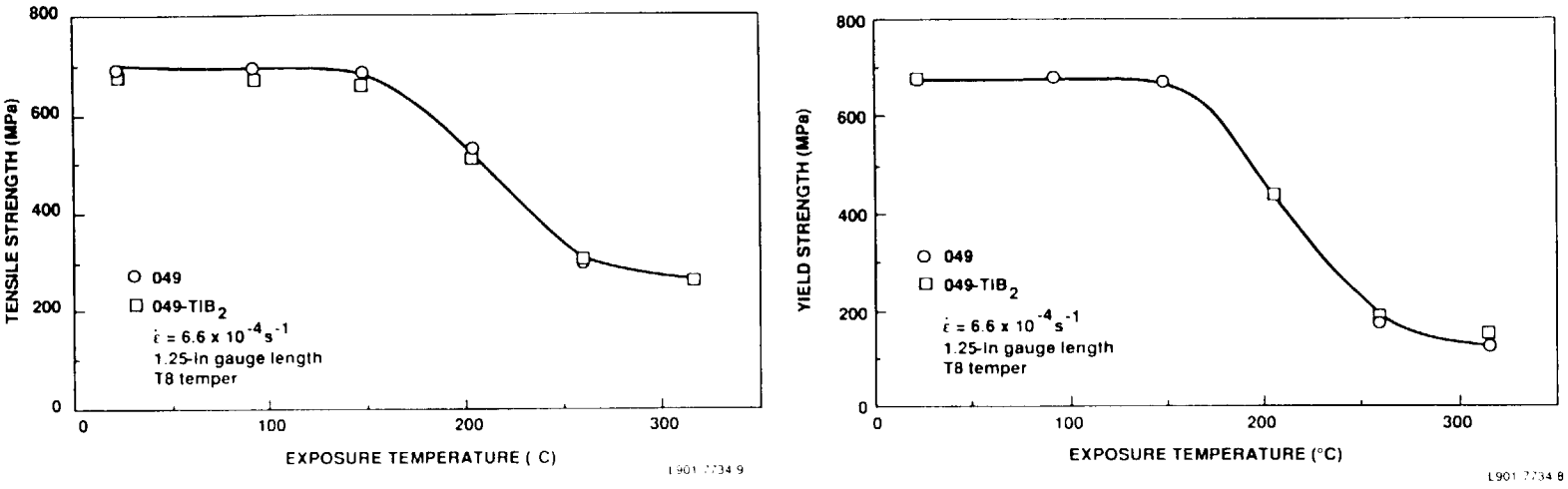

(a) (b)

FIG. 5. Strength at room temperature after 100 h at temperature: (a) ultimate tensile strength, (b) tensile yield strength.

Discussion

The strength-ductility combinations of alloy 049-TiB_2 in the T3 and T8 tempers compare favorably with those of other aluminum-lithium MMCs. In fact, the combination of 410 MPa YS, 529 MPa UTS, and 6.5% elongation observed for 049-TiB_2 in the T3 temper is competitive with values reported for 8090-10 vol% SiC and 8090-11 vol% B_4C in the peak-aged tempers (7,8). In addition, equally attractive properties are obtained after 2 hours aging at 160°C (Fig. 2b), a more stable condition. Both 049 and 049-TiB_2 undergo reversion on aging from T3 to T8 tempers. Reversion of Weldalite™ 049 without cold work (i.e., on aging from the T4 to T6 temper) has also been observed (3) and was studied by Gayle et al. (9), who observed dissolution of fine δ' and GP zones from the T4 temper, leaving coarser GP zones as the only major strengthening precipitate in the "T4 reversion" temper. These phases were also observed by Kumar et al. (10) for Weldalite™ 049 in the early stages of reversion from the T3 temper, and it is likely that the "T3 reversion" of 049 and 049-TiB_2 results from dissolution of δ' and GP zones.

The TiB_2 particle size is too large (~ 1 μm) and the volume fraction too low (~ 4%) to increase strength by dispersion (Orowan) strengthening. England et al. (11) plotted theoretical critical resolved shear-stress values, determined from the Orowan equation, vs particle radius for three particle volume fractions, and found that little increase in strength (i.e., only up to ~ 20 MPa) could be expected for particles with a radius of $\geq$ 0.1 μm at volume fractions up to 15%. Particles with radii larger than 0.1 μm have been shown to contribute to strengthening at high loadings (i.e., in excess of 25% by

volume) by matrix constraint (12). This is an important strengthening mechanism in sintered (i.e., cemented) carbides and cermets, where the hard phase occupies 85 - 95% of the volume, but clearly is not an operative strengthening mechanism in 049-TiB_2.

Aging kinetics for 049-TiB_2 are accelerated with respect to those in 049, but the peak strength values are similar for both alloys. An increased dislocation density resulting from a mismatch in the coefficient of thermal expansion (CTE) between the matrix and the reinforcement phase can alter the matrix aging kinetics and, in some cases, increase the strength of the MMC. This behavior was shown for aluminum alloys 2124 reinforced with SiC whiskers (13) and 6061 reinforced with B_4C particles (14). Since the CTE of TiB_2 is roughly one-third that of aluminum, the increase in aging kinetics for 049-TiB_2 likely results from enhanced diffusion associated with an increase in the matrix dislocation density. Nevertheless, the peak strength values obtained for 049 and 049-TiB_2 are the same.

049 and 049-TiB_2 both show excellent warm-temperature properties compared with leading conventional aluminum alloys intended for service in that regime, such as 2219 (15). Alloy 049 retains a YS of 365 MPa after a 0.5-h exposure at 260°C, which is only slightly lower than the typical room-temperature YS of 2219-T87, 393 MPa (16). Exposure to temperatures below 149°C causes little change in the tensile properties of 049 or 049-TiB_2 aged for 24 h at 160°C, since further "aging" at the lower temperatures does not significantly affect the strengthening precipitates. A decrease in tensile UTS and YS is observed above 149°C. The brightfield TEM micrograph of 049 after 100 h at 260°C shows the presence of "coarse" T_1-type precipitates (Fig. 6),

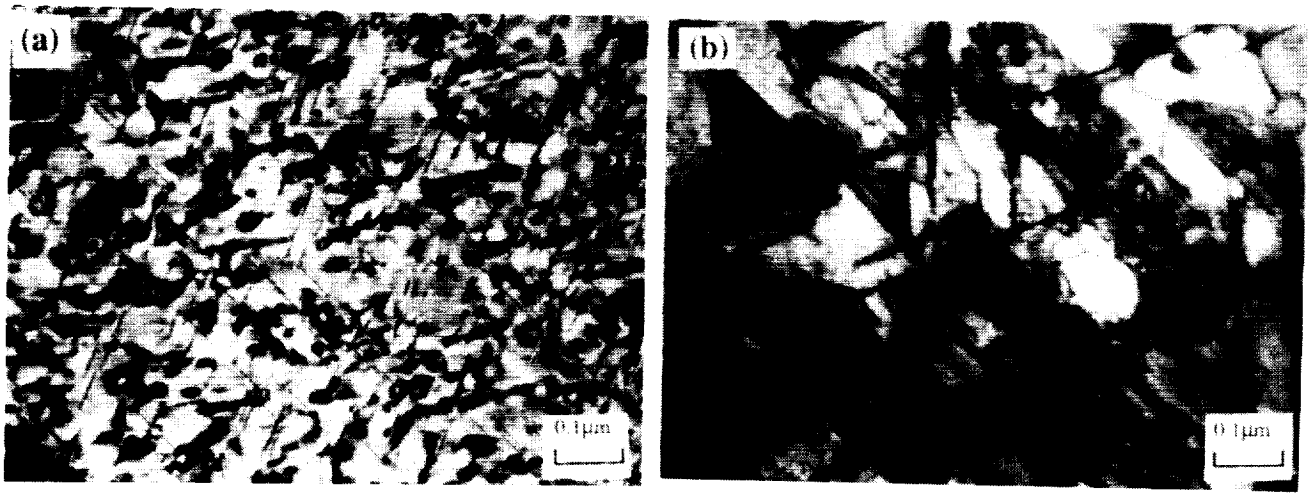

FIG. 6. TEM brightfield micrographs: (a) 049-T8 and (b) 049-T8 after 100 h at 260°C.

which are about six times thicker (Fig. 6b) than those in the T8 temper (Fig. 6a). Thus, as might be expected, precipitate coarsening is partially responsible for the decrease in room-temperature properties of 049 after exposure to temperatures above 149°C for 100 h. The slightly steeper decrease in tensile properties occurring in 049-TiB_2 after 100-h exposures may result from the increased aging kinetics associated with the TiB_2 reinforcement. Although no increase in strength results from reinforcement of Weldalite™ 049 at low volume fractions, this MMC could be useful in applications where stiffness is a critical design consideration. Also, it is important to note that even with the loss in ductility associated with the agglomerated TiB_2, the Weldalite™ 049 matrix is forgiving enough to produce a potentially viable MMC with good T3 properties. Thus, Weldalite™ 049 should be considered for the matrix of future high-strength MMCs.

Conclusions

1. Both 049 and 049-TiB_2 show very attractive warm-temperature properties (e.g., 625 MPa yield strength at 150°C after 100 h at temperature).
2. Weldalite™ 049 reinforced with a nominal 4 v% TiB_2 shows an ~ 8% increase in modulus and a good combination of strength (529 MPa UTS) and ductility (6.5%) in the T3 temper.
3. The high ductility of Weldalite™ 049 in the naturally aged and underaged tempers makes the alloy a good, high-strength matrix for ceramic reinforcement.

Acknowledgement

This work was supported by NASA Contract #NAS1-18531, and the authors wish to thank Contract Monitor, W. Brewer, for his support. We would also like to thank F.H. Heubaum and L.S. Kramer for the fabrication of the materials, W. Precht and K. Moore for their assistance in performing tensile testing, L. Friant for the ultrasonic modulus measurements, and members of the Composites Group at Martin Marietta Laboratories for providing the TiB_2 particles made by the XD™ process.

References

1. A.P. Divetcha, S.G. Fishman, and S.D. Karmarkar, J. Metals, 33, 12 (1981).
2. F.H. Froes and J.R. Pickens, J. Metals, 36, 14 (1984).
3. J.R. Pickens, F.H. Heubaum, L.S. Kramer, and T.J. Langan, in Proc. 5th Int. Al-Li Conf., T.H. Sanders and E.A. Starke, eds., MCE, London, p. 1397 (1989).
4. T.J. Langan and J.R. Pickens, ibid. Ref. 3, p. 691.
5. K.K. Sankaran and N.J. Grant, in Aluminum-Lithium Alloys, TMS-AIME Conference Proc., T.H. Sanders, Jr., and E.A. Starke, Jr., eds., Warrendale, PA, p. 206 (1981).
6. A.R.C. Westwood, Metall. Trans., 19A, 749 (1988).
7. J. White, I.R. Hughes, T.C. Willis, and J.M. Jordan, J. Physique (Paris) 48, C3, C-347 (1987).
8. J. White, I.G. Palmer, I.R. Hughes, and S.A. Court, ibid. Ref. 3, p. 1635 (1989).
9. F.W. Gayle, F.H. Heubaum, and J.R. Pickens, ibid. Ref. 3, p. 701.
10. K.S. Kumar, S.A. Brown and J.R. Pickens, Scripta Metall.et Mat., 24, 1245 (1990).
11. R.O. England, J.R. Pickens, K.S. Kumar, and T.J. Langan, in Dispersion Strengthened Al Alloys, Y-W Kim and W.M. Griffith, eds., TMS, Warrendale, PA, p. 371 (1988).
12. L.J. Broutman and R.H. Krock (eds.), Modern Composite Materials, Addison-Wesley Publishing Co., NY (1969).
13. T. Christman and S. Suresh, Acta Metall., 36, 1961 (1988).

14. T.G. Nieh and R.F. Karlak, Scripta Metall., 18, 25 (1984).

15. Metallic Materials and Elements for Aerospace Vehicle Structures, Mil-Handbook-5D, Vol. 1, p. 3-156 (1986).

16. Aluminum Standards and Data 1984, Aluminum Assoc., Washington, DC (1984).

APPENDIX A

WELDABILITY OF WELDALITE™ 049 WITH AND WITHOUT TiB_2 REINFORCEMENT

An internally funded evaluation of the weldability of Weldalite™ 049 is currently under way at Martin Marietta Laboratories, funded by Martin Marietta Corporation (see Pickens et al.[1], Kramer et al.[2] and Pickens[3]). In addition, weld parameter development is being conducted at Martin Marietta's operating companies under both IR&D and Advanced Launch System program office funding.

The goal of the study detailed herein is to assess the effects of TiB_2 reinforcement and parent alloy Li content on the weldability of Weldalite™ 049-type alloys. Welding trials were performed by G. Doherty at Martin Marietta Aero & Naval Systems using either AC or DC polarity gas tungsten arc (GTA) welding according to the procedures described in Tables A-1 and A-2. The welding was performed under conditions of high restraint on 5-cm (2-in.)-wide x 25.4-cm (10-in.)-long plates machined from the 0.952-cm (0.375-in.) extruded bar parallel to the extrusion direction. A 37.5° bevel was machined on the center edge of the extruded bar. "Cut rod" filler wire, measuring 0.317 cm x 0.317 cm x 50.8 cm (0.125 in. x 0.125 in. x 20 in.) long, was machined from alloys 049(1.3)[heat 116], 049(1.9), and 049-TiB_2. Commercially obtained 2319 filler wire was also used.

---

(1) J.R. Pickens, F.M. Heubaum, T.J. Langan, and L.S. Kramer, In Proc. of the Fifth Int. Al-Li Conf., T.H. Sanders and E.A. Starke, eds., Material and Component Eng. Pub. Ltd., p. 1397 (1989).

(2) L.S. Kramer, F.H. Heubaum, and J.R. Pickens, ibid., p. 1415.

(3) J.R. Pickens, "Recent Developments in the Weldability of Lithium-Containing Aluminum Alloys," J. Mater. Sci., Vol. 25, pp. 3035-3047, (1990).

Table A-1

Alloy/Filler Materials Used in Welding Trials

Parent Alloy	Filler Alloy	Polarity
049(1.3) [heat 072]	049(1.3) [heat 116]	DC
	2319	DC
	049(1.9)	DC
	049-TiB_2	DC
	049(1.3) [heat 116]	AC
	049-TiB_2	AC
049 TiB_2	049(1.3) [heat 116]	DC
	2319	DC
	049-TiB_2	DC
	049-TiB_2	DC
049(1.9)	049(1.9)	DC
	2319	DC

Both the plates and filler wire were "chem-milled" prior to welding according to the following procedure: (1) chem-mill in 30% NaOH aqueous solution, (2) rinse in distilled water, (3) desmut in 30% HNO_4 aqueous solution, (4) rinse in distilled water and air dry. Both were then stored in a dessicator until welding. The welding equipment and set-up procedures are outlined in Table A-2. All plates were welded in the T8 temper; the welding sequence used is shown in Fig. A-1.

After welding, the weld bead was machined flush on 20 cm (8 in.) of each weldment, and the welds were radiographed. Tensile specimens were machined from each dressed weldment, naturally aged for about 2000 h, and tested.

TABLE A-2 EQUIPMENT / SETUP PROCEDURES FOR WELDING

POWER SOURCE	MILLER SYNCROWAVE 500 AC/DC
ELECTRODE	EWTH 2% 1/8" DIAMETER
CUP SIZE	5/8"
SHIELD GAS	100 % HELIUM 60 CFH
CURRENT	DIRECT CURRENT STRAIGHT POLARITY
	(REFERENCE INDIVIDUAL CONTROL SHEETS)

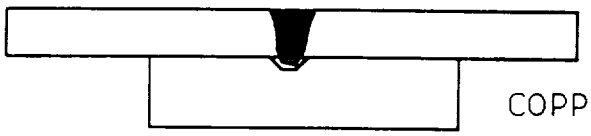

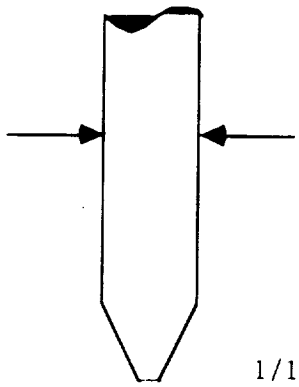

1/16" FLAT GROUND ON END OF ELECTRODE

ELECTRODE CONFIGURATION

ALUMINUM LITHIUM WELDING

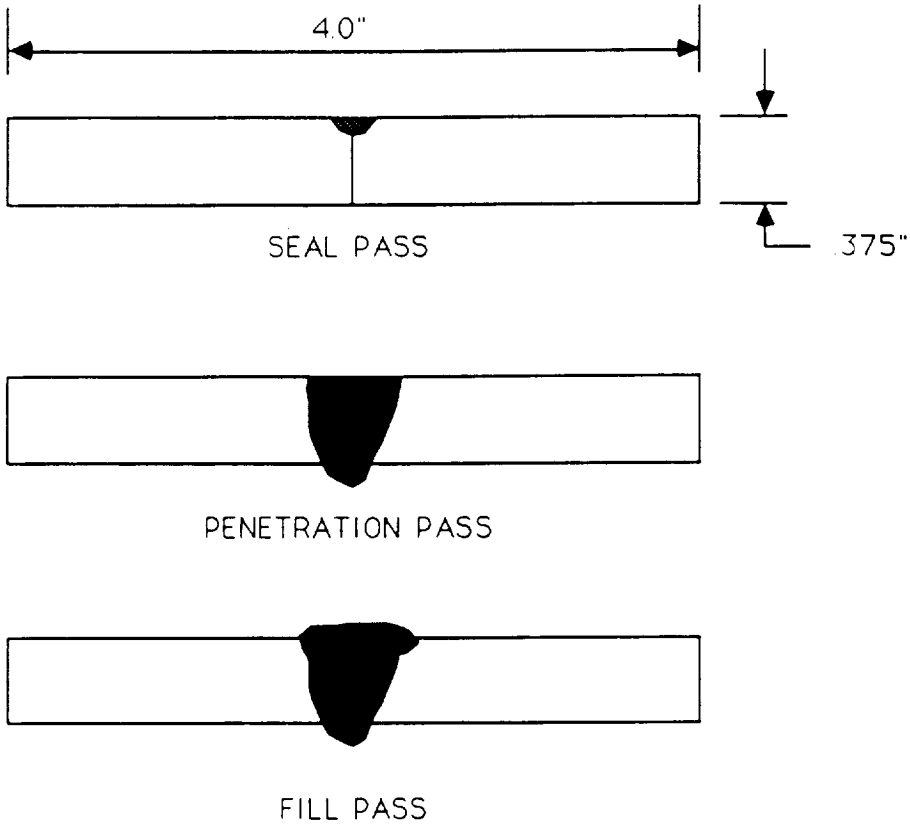

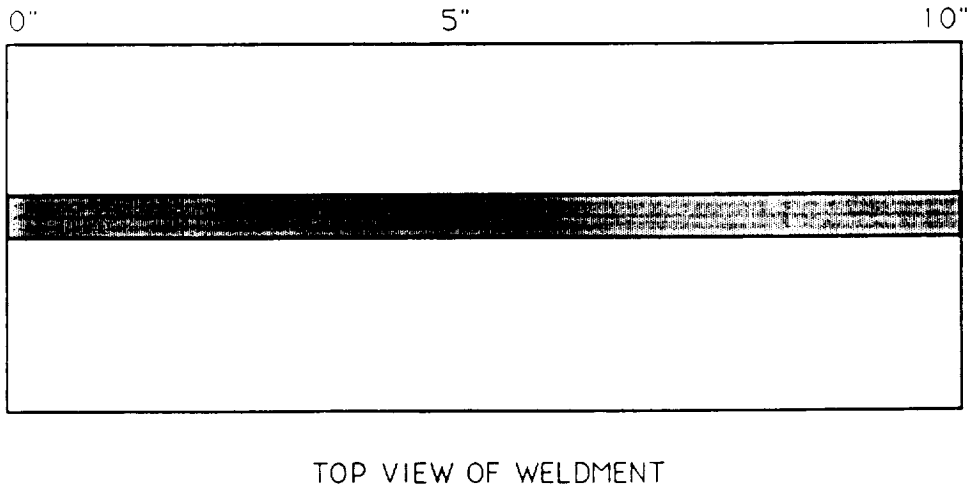

Fig. A-1 Schematic showing welding sequence.

Weldability was evaluated for Weldalite™ 049-type alloys at Li levels of 1.3 and 1.9 wt%. Alloys 049(1.3) and 049(1.9) were welded using cut-rod filler (i.e., parent alloy) of alloys 049(1.3) and 049(1.9) and conventional 2319 filler.

Weldments of 049(1.3) parent with 049(1.3) and 049(1.9) filler had similar tensile properties (Table A-3), with UTS values of 311 MPa (45.1 ksi) and 306 MPa (44.4 ksi), respectively. Thus, increasing the Li level in the weld zone did not change weldment strength for the experimental conditions investigated. Weldment strengths were also similar for high- and low-lithium (i.e., 049(1.9) and 049(1.3)) parent plates that were welded with 2319 and 049(1.3) filler. The lowest ductility was observed for 049(1.9) parent welded with 049(1.9) filler.

The weldment strengths were higher than those typically attained for the strongest weldable 2XXX alloys, but not as strong as those obtained on Weldalite™ 049 reported elsewhere.[1,2] For example, these investigators routinely attained weldment strengths of 340-345 MPa (49-50 ksi). In addition, lowering the Cu content of Weldalite™ 049 from 6.3 to 4.75 wt% leads to increased weldment ductility.

Weldment strength was also determined for alloys 049(1.3) and 049(1.3)-TiB_2 welded using reinforced and non-reinforced filler. The presence of TiB_2 in the filler or the parent metal had little effect on weldment UTS (Table A-4). Elongations to failure were somewhat lower for all weldments made with 049(1.3)-TiB_2 parent material.

AC GTA welding was performed with the reinforced filler to determine if the fluctuating polarity would break up any agglomerated TiB_2 clumps in the

Table A-3

As-Welded Tensile Properties for Manual GTA Weldments of Weldalite™ 049-Type Alloys at Two Lithium Levels

(T8 temper, NA > 2000 h)

Alloy	Filler	UTS* (ksi)	UTS* (MPa)	Apparent YS (ksi)	Apparent YS (MPa)	%El (1 in.)
049(1.3) [heat 072]	049(1.3) [heat 116]	45.1	(311)	37.5	(259)	2.1
	2319	44.5	(307)	36.1	(245)	2.2
	049(1.9)	44.4	(306)	37.8	(261)	1.9
049(1.9)	2319	46.0	(317)	37.6	(259)	3.2
	049(1.9)	42.2	(291)	39.6	(273)	0.7
2219 T81†	2319	38.0	(262)	26.0	(179)	3.0

* Weld bead dressed

† Typicals

Table A-4

As-Welded Tensile Properties for Manual GTA Weldments of TiB_2-Reinforced vs Non-Reinforced Weldalite™ 049

(T8 temper, NA >2000 h)

Alloy	Filler	UTS* (ksi)	UTS* (MPa)	Apparent YS (ksi)	Apparent YS (MPa)	%El (1 in.)
049(1.3) [heat 072]	049(1.3) [heat 116]	45.1	(311)	37.5	(259)	2.1
	2319	44.5	(307)	36.1	(249)	2.2
	049-TiB_2	46.0	(317)	39.1	(270)	1.9
049-TiB_2	049 [heat 116]	43.9	(303)	42.5	(293)	0.4
	2319	44.5	(307)	39.8	(274)	0.9
	049-TiB_2	45.8	(316)	44.3	(305)	0.4
2219 T81	2319	38.0	(262)	26.0	(179)	3.0†

* Weld bead dressed

† Typicals

weld pool. No change in UTS was observed between the weldments fabricated using AC or DC polarity (Table A-5). However, the measured ductility increased for AC as opposed to DC polarity for 049-TiB_2 welded with 049-TiB_2 filler metal. This change could be the result of a decrease in agglomeration of TiB_2 particles in the weld zone, or it could be due in part to the change in the size of the fusion zone between AC and DC weldments.

Table A-5

As-Welded Tensile Properties of AC and DC GTA Weldments of TiB_2-Reinforced and Non-Reinforced Weldalite™ 049 Alloys

(T8 temper, NA > 2000 h)

Alloy	Filler	AC/DC	UTS* (ksi)	UTS* (MPa)	Apparent YS (ksi)	Apparent YS (MPa)	%El (1 in.)
049 (1.3) [heat 072]	049 (1.3) [heat 116]	DC	45.1	(311)	37.5	(259)	2.1
		AC	44.9	(310)	39.0	(269)	1.7
049 (1.3) [heat 072]	049-TiB_2	DC	46.0	(317)	39.1	(270)	1.9
		AC	43.7	(301)	39.1	(270)	1.9
049-TiB_2	049-TiB_2	DC	45.8	(316)	44.3	(305)	0.5
		AC	44.1	(304)	41.9	(289)	1.3

* Weld bead dressed

Concluding Remarks. This preliminary assessment of the weldability of TiB_2-reinforced and non-reinforced Weldalite™ alloys revealed no propensity for hot cracking under conditions of high restraint. This result is significant, because hot cracking has been reported for all other leading aluminum-lithium alloys (i.e., 2091, 2090, and 8090[4,5]) welded with certain conventional filler alloys. In addition, 8090[5] weldments made with parent alloy filler are particularly sensitive to hot cracking. The strengths for Weldalite™ parent welded with parent filler obtained in the present study were higher than those for alloys used in launch systems, such as alloys 2219 and 2014 welded with 2319 and 4043 fillers, respectively. Even higher values have been obtained at Martin Marietta Manned Space Systems by variable polarity plasma arc welding (e.g., 54 ksi (372 MPa) mean tensile strength).[3]

4) R.P. Martukanitz, C.A. Natalie, and J.O. Knoefel, J. Metals, pp. 38-42 (1987).

5) M.F. Gittos, Report #7944.01/87/556.2, The Welding Inst., Abingdon, Cambridge, UK (1987).

APPENDIX B

EFFECT OF Li LEVEL, ARTIFICIAL AGING, AND TiB_2 REINFORCEMENT ON THE FRACTURE TOUGHNESS OF WELDALITE™ 049-TYPE ALLOYS

Plane-strain fracture toughness (K_{IC}) was evaluated for Weldalite™ 049 with and without TiB_2 reinforcement. For the non-reinforced variant, changes in toughness were measured for various aging conditions and lithium levels.

Toughness testing was carried out on fatigue precracked compact tension (CT) specimens at 24°C (75°F), as per ASTM standard E-399, by Westmoreland Mechanical Testing and Research, Inc., Youngstown, PA. Specimens were machined in both the L-T and the T-L orientations, with the standard 1.27-cm (0.500-in) geometry, 0.927-cm (0.365-in.) thick.

Toughness was measured as a function of aging time at 160°C (320°F) for the two Weldalite™ 049(1.3) heats, 049(1.3) [heat 116] and 049(1.3) [heat 072] (Table B-1). The composition of these heats differed only in that 0.03 wt% Ti was added to 049(1.3) [heat 116] as an additional grain refiner. Both heats showed a decrease in toughness with increasing aging time, although toughness values for heat 116 were significantly higher than those for heat 072. This greater toughness may be due to a subtle change in the grain size resulting from the presence of Ti or, alternatively, to differences in texture or substructure formed during extrusion. K_{IC} and K_q values are quite promising: 22.5 MPa$\sqrt{m}$ (20.5 ksi$\sqrt{in}$) at a yield strength of 700 MPa (101.5 ksi), and 35.7 MPa$\sqrt{m}$ (32.5 ksi$\sqrt{in}$) at a yield strength of 565 MPa (82.0 ksi), respectively.

An extensive temper development program is currently under way at both Martin Marietta Laboratories and Reynolds Metals Co. to optimize temper and microstructure for the best combinations of toughness and strength. In fact, a reduction in the Cu content of Weldalite™ 049 to 4.75 wt% has already been shown to improve K_{IC} on both extrusions and rolled plate. For example,

Table B-1

Effect of Aging Time on the Fracture Toughness* of Weldalite™ 049

Alloy**	Aging Time at 160°C (320°F) (h)	Orientation	K_{IC} ksi√in	K_{IC} (MPa√m)	K_q ksi√in	K_q (MPa√m)	YS ksi	YS (MPa)
049(1.3) [heat 072]	6	L-T	24.8	(27.3)	--		86.0	(593)
	20	L-T	14.8	(16.3)	--		93.8	(647)
	24 (T8)	L-T	13.2, 12.0	(14.5, 13.2)	--		98.0	(676)
		T-L	11.4, 11.1	(12.5, 12.2)	--		--	--
049(1.3) [heat 116]	6	L-T	--		32.5†	(35.7)	82.0	(565)
	20 (T8)	L-T	20.5	(22.5)	--		101.5	(700)

* 1.27-cm (0.500-in) (CT) compact fracture toughness specimens, 0.927-cm (0.365-in) thick, tested at 24°C (75°F)

** 0.953-cm x 10.2-cm (0.375-in x 4-in) extruded bar, WQ, stretched

† Invalid test as per ASTM E-399

Heubaum and Pickens,[1] using specimens in the L-T orientation from extruded Weldalite™ 049 bar containing about 5.0% Cu, obtained K_{IC} values of 24.2, 34.6, and 50.6 MPa$\sqrt{m}$ (22, 31.5, and 46 ksi$\sqrt{in}$) at yield strength levels of 717, 621, and 414 MPa (104, 90 and 60 ksi), respectively.

The effect of Li level on the K_{IC} of Weldalite™ 049-type alloys was determined for three variants at nominally the same strength level (Table B-2). As shown in Section I of this report, increasing the lithium content of Weldalite™ 049 decreases the maximum strength obtained in the peak-aged temper. Therefore, to compare toughness at similar strengths, we aged both of the 049(1.3) heats to an underaged temper (6 h at 160°C (320°F)) and alloys 049(1.6) and 049(1.9) to their peak-aged (comparable strength) tempers 34 h at 160°C (320°F)) (Table B-2). Under these conditions, the K_{IC} values for 049(1.6) and 049(1.9) were about 30% lower than the lowest K_{IC} value for 049(1.3). However, since grain boundary microstructure may play an important role in the fracture of aluminum-lithium alloys -- and is more a function of artificial aging history than alloy strength per se -- we also compared toughness values for the three lithium levels in the peak-aged temper. The low toughness for heat 049 (heat 072) is unfortunate and these studies should be repeated with more representative material that also includes alloys with lower Cu content.

Reinforcement of Weldalite™ 049(1.3) with TiB_2 particles produced a similar toughness (Table B-3) comparable to that of alloy 049(1.3) [heat 072], but lower than that for 049 [heat 116] in the peak-aged temper.

(1) F.H. Heubaum and J.R. Pickens, Presentation by J.R. Pickens at Al-Li V, Williamsburg, VA, Mar. 29, 1989.

Table B-2

Effect of Lithium Level on the Fracture Toughness* of Weldalite™ 049

Alloy	Weight % Li	Aging Time at 160°C (320°F) (h)	K_{IC} ksi√in	(MPa√m)	K_q ksi√in	(MPa√m)	YS ksi	(MPa)
049 (1.9)	1.9	34 (T8)	16.8†	(18.5)	--		78.0	(538)
049 (1.6)	1.6	34 (T8)	17.4†	(19.1)	--		84.2	(579)
049 (1.3) [heat 072]	1.3	24 (T8)	12.6†	(13.8)	--		98.0	(676)
		6	24.4	(26.8)	--		86.0	(593)
049 (1.3) [heat 116]	1.3	20 (T8)	20.5	(22.5)	--		101.2	(698)
		6			32.5	(35.7)††	82.0	(565)

* 1.27-cm (0.500-in) compact fracture toughness specimens, 0.927-cm (0.365-in) thick, tested at 24°C (75°F)

** 0.953-cm x 10.2-cm (0.375-in x 4-in) extruded bar, WQ, stretched

† Mean of two tests

†† Invalid test as per ASTM E-399

Table B-3

Fracture Toughness* for TiB_2-Reinforced
vs Non-Reinforced Weldalite™ Alloys in the T8 Temper

Alloy**	Orientation	K_{IC} ksi√in	K_{IC} (MPa√m)	YS ksi	YS (MPa)
049(1.3) [heat 116]	L-T	20.5	(22.5)	101.2	(698)
049(1.3) [heat 072]	L-T	12.6†	(13.8)	98.0	(676)
	T-L	11.2†	(12.3)		
049(1.3)-TiB_2	L-T	12.4†	(13.6)	94.2	(650)
	T-L	10.8†	(11.9)		

* 1.27-cm (0.500-in) compact fracture toughness specimens, 0.375-in thick, tested at 24°C (75°F)

** From 0.953 cm x 10.2 cm (0.375-in x 4-in) extruded bar

† Mean of two tests

APPENDIX C

EFFECT OF Li LEVEL, ARTIFICIAL AGING, AND TiB_2 REINFORCEMENT ON THE MODULUS OF WELDALITE™ 049

The dynamic Young's Modulus (E) was determined for alloys 049(1.3)[heat 072], 049(1.9), and 049(1.3)-TiB_2 in the T3 temper and after aging at 160°C (320°F) for 0.08, 0.25, 1.5, 6, 24, and 100 h. Measurements for each alloy were made on a single 0.953-cm (0.375-in) cube to reduce scatter from microstructural inhomogeneities. Both shear and transverse wave velocities were measured for the L, LT, and ST directions by a pulse-echo technique, detailed in ASTM Standard Recommended Practice (ASTM E494-75). These velocities were then used to calculate modulus according to equations in the Appendices of the ASTM standard.

Figures C1-C3 show the change in E with aging time at 160°C (320°F) for the three alloys. It is clear from these plots that aging has a minor, but measurable, influence on the E of alloys 049(1.3) and 049(1.9): E decreases by ~2.5% for 049(1.3) and 049(1.9) during the initial stages of artificial aging (Figs. C1 and C2). This decrease in E generally follows the strength reversion (Fig. C4). On further aging beyond the reversion well, E increases, peaks between 24 and 100 h, and then decreases again as the alloys over-age. The slightly higher, although not statistically significant, modulus in the T8 than in the T3 temper is consistent with the presence of the high-modulus T_1 phase in the T8 temper. A similar, but more subtle, change in E was observed on aging for the TiB_2-reinforced variant (Fig. C3) that also follows the aging curve (Fig. C5).

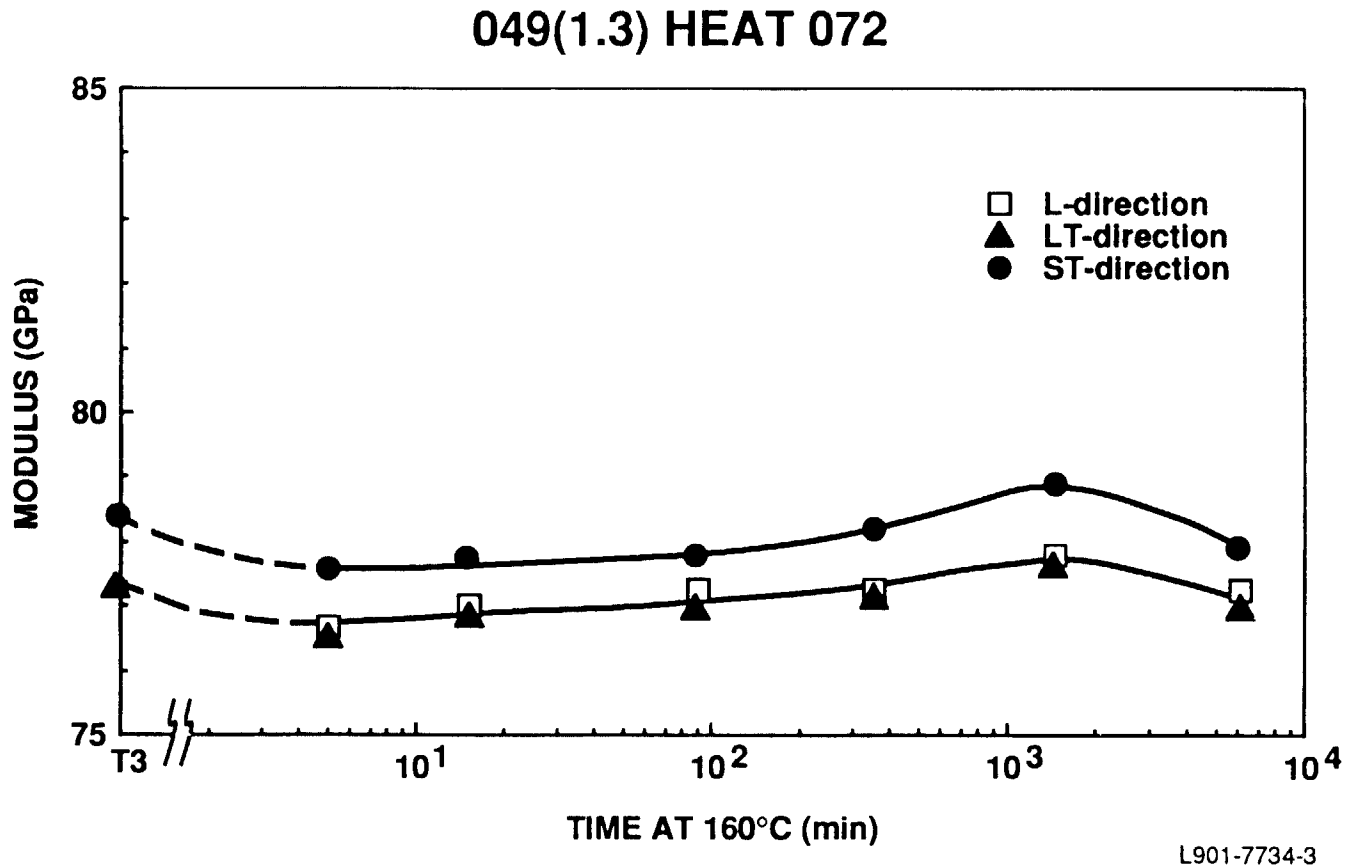

Fig. C-1 Young's Modulus (E) vs. aging time at 160°C for 049(1.3)[heat 072] for three directions relative to the extrusion direction of the bar.

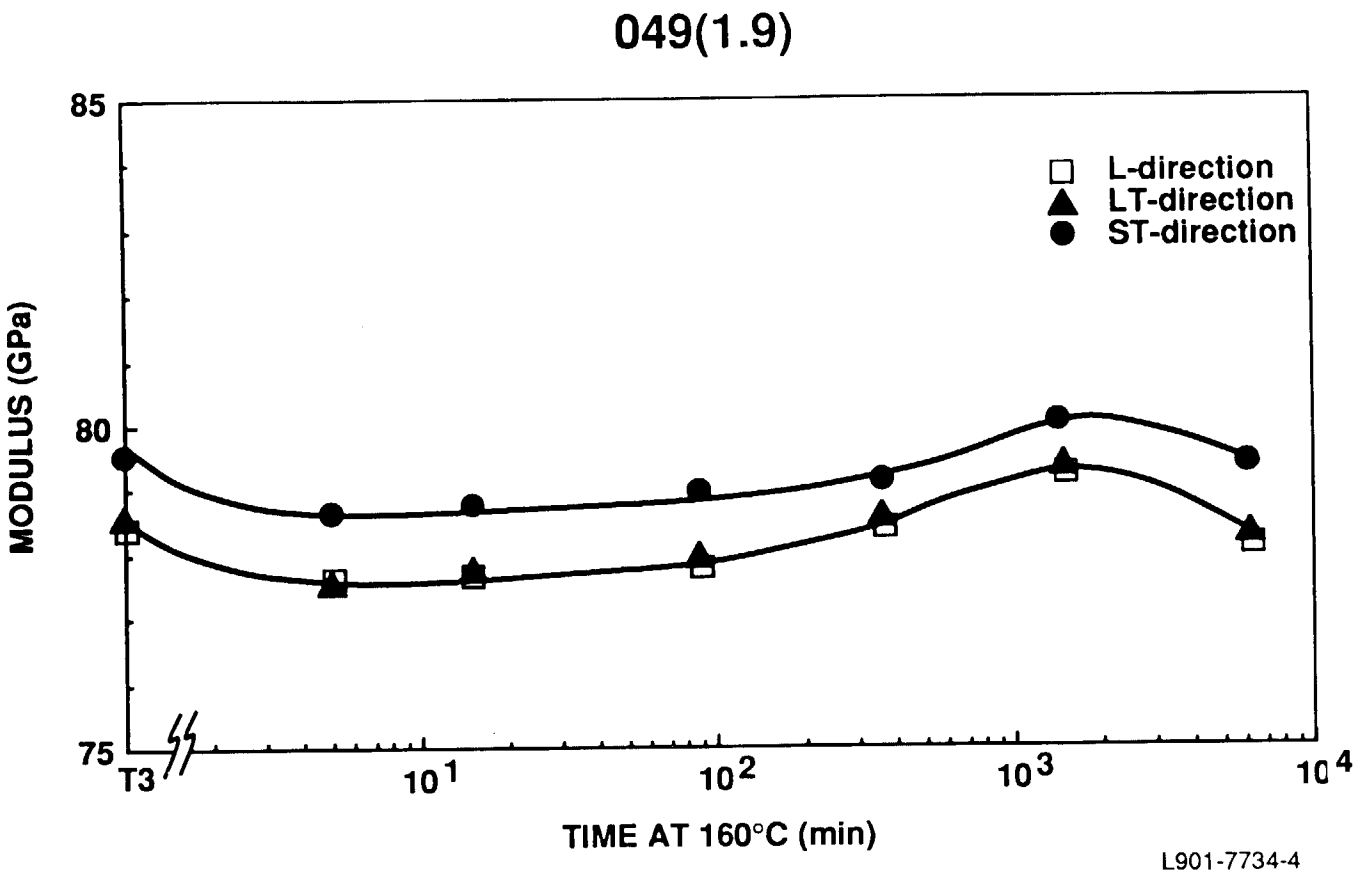

Fig. C-2 Young's Modulus (E) vs. aging time at 160°C for 049(1.9) for three directions relative to the extrusion direction of the bar.

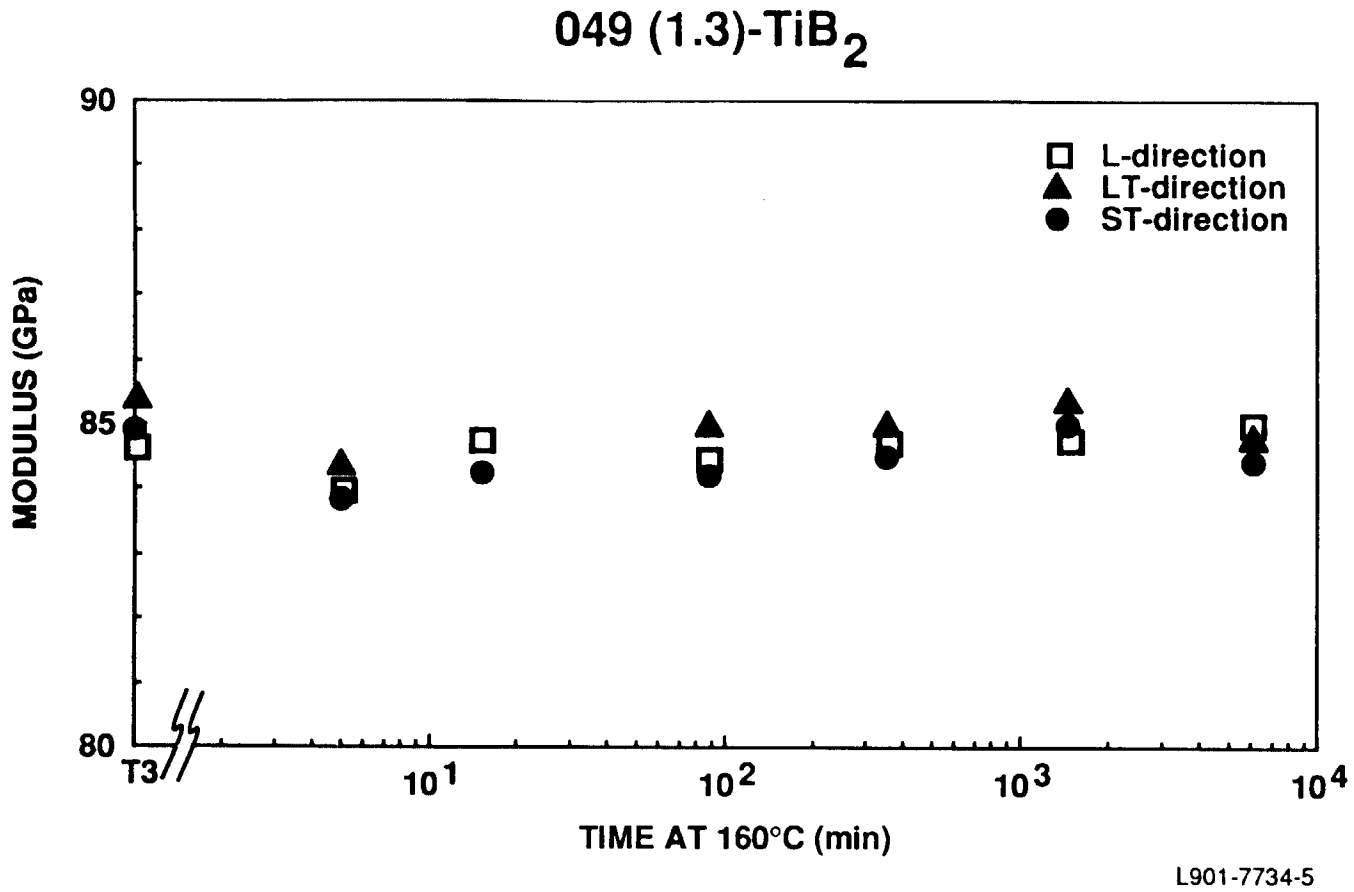

Fig. C-3 Young's Modulus (E) vs. aging time at 160°C for 049-TiB_2 for three directions relative to the extrusion direction.

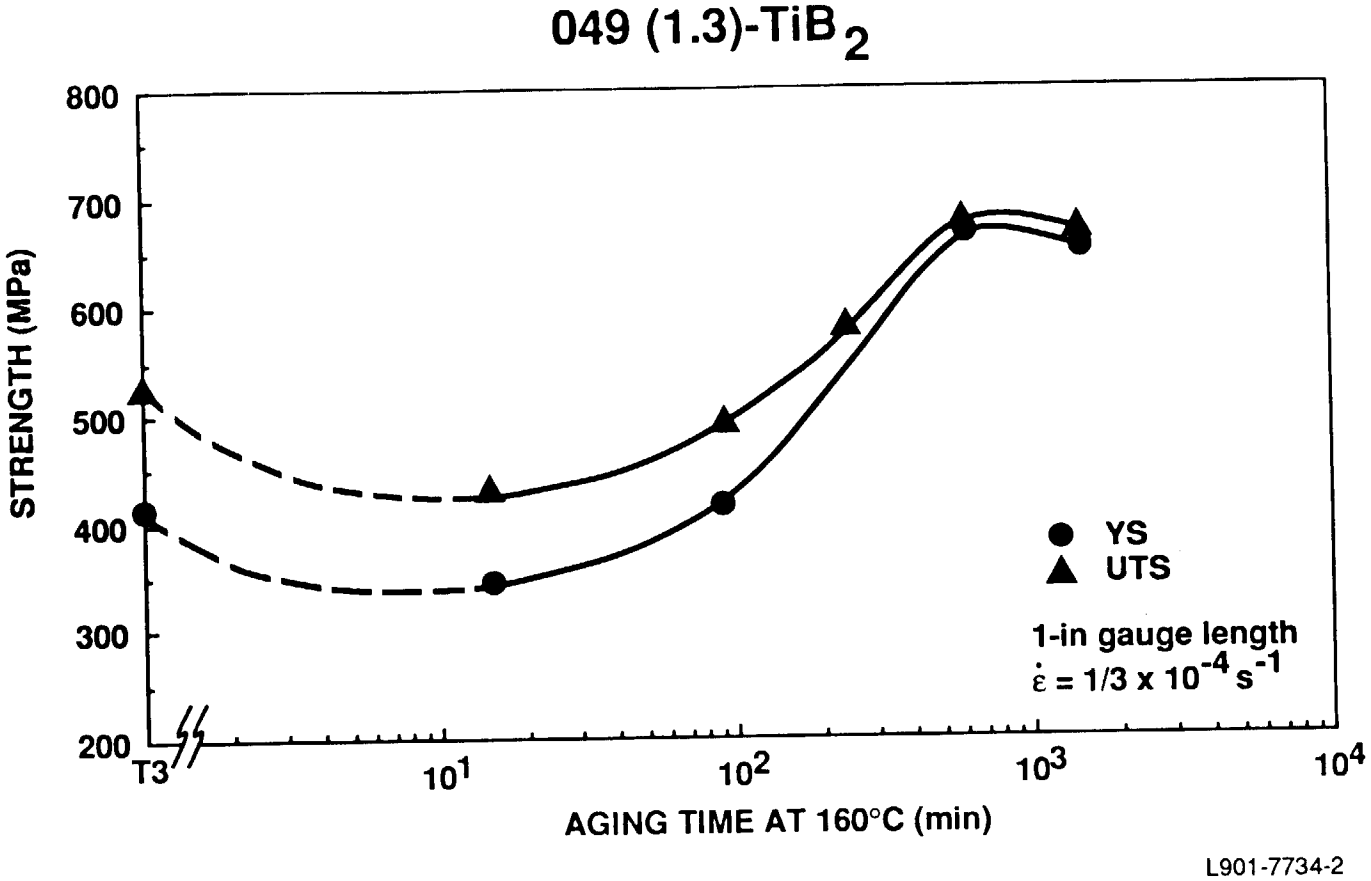

Fig. C-4 Tensile yield strength (YS) and ultimate tensile strength (UTS) vs. aging time for 049(1.3)[heat 072].

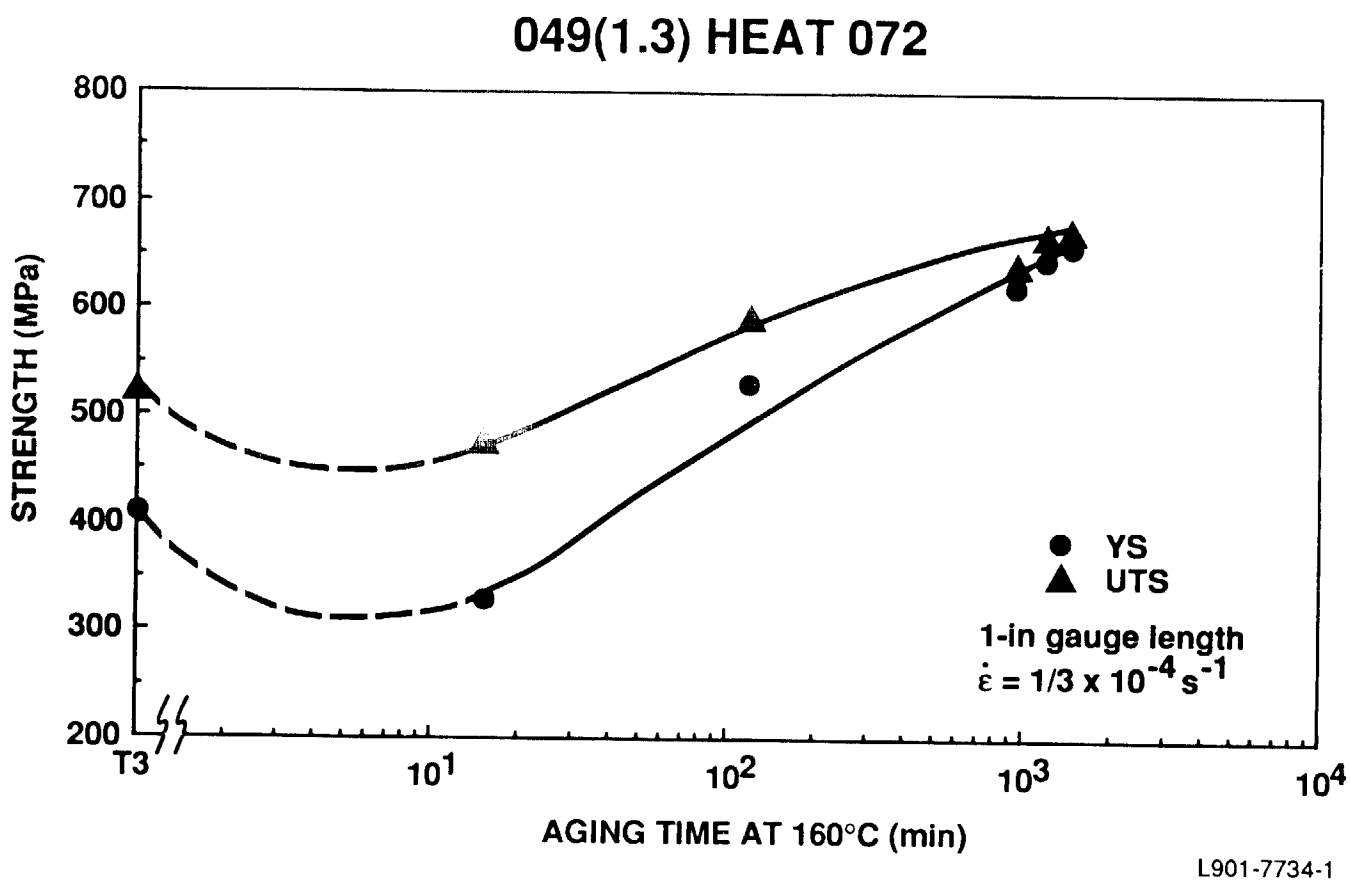

Fig. C-5 Tensile yield strength (YS) and ultimate tensile strength (UTS) vs. aging time for 049-TiB_2.

O'Dowd et al. [1] showed that E is dependent on artificial aging time for 2090-type Al-Li-Cu alloys, and attributed variations in E to precipitation of the T_1 (Al_2CuLi) and δ' (Al_3Li) phases. The modulus of δ' was estimated to be 106 GPa[2], and that for T_1 170 GPa.[2] O'Dowd et al.[1] concluded that the T_1-phase contributes more to E than δ'. Weldalite™ 049 (i.e., alloy 049(1.3)) has approximately the same modulus in the T3 and T8 tempers. In the T3 temper, 049(1.3) is strengthened by the δ'-phase and GP zones, with Li and Cu atoms in supersaturated solid solution; in the T8 temper, the alloy is strengthened primarily by T_1-type precipitates. Thus, for 049(1.3), the contribution to E from δ' and GP zones, plus Li and Cu atoms in solid solution is about the same as that from the uniform T_1-type distribution in the T8 temper.

A small amount of anisotropy was observed for E in the ST vs the L and LT directions for 049(1.3) and 049(1.9). A variation with orientation was also observed by O'Dowd et al. [1] for 2090-type alloys, but they dismissed it as being within the experimental error of their technique. The relative difference in E between orientations for Weldalite™ 049 alloys was approximately 1 GPa (0.15 Msi). However, the trend followed between directions is consistent for all measurements and is the same as that observed by O'Dowd et al.[1]. Thus, it appears that E is slightly dependent on

---

(1) M.E. O'Dowd, W. Ruch, and E.A. Starke, Jr., J. Physique (Paris), 48, C3, pp. C-565-576 (1987).

(2) W. Muller, E. Bubeck, and V. Gerold, in Al-Li Alloys III, Inst. of Metals, London, p. 435 (1986).

direction, with E in the ST direction being a higher (78.9 GPa) than in the L (77.8 GPa) or LT (77.6 GPa).

In the T3 temper, E for the high-lithium variant, 049(1.9), was 1.5% higher than that for 049(1.3) in each of the three orientations evaluated. In the near-peak-aged temper (24 h at 160°C), the increase in E with increasing lithium content was slightly greater for the L and LT orientations than for the ST orientation: the L and LT orientations showed approximately a 2% increase, while the ST orientation showed an increase of 1.5%. Thus, a 0.6 wt% increase in lithium results in a 1.5 to 2% increase in E, the equivalent of a 3 to 4% increase per wt% lithium, which compares favorably with the results of Peel. [3] He showed that E increases by approximately 3.5% for each wt% increase in lithium for a number of commercial Al-Li-Cu, Al-Li-Cu-Mg and Al-Mg-Li alloys. [3] However, this is lower than the 6% increase in E per 1 wt% Li observed for Al-Li binary alloys by Sankaran and Grant.[4] The reason for the slight difference in the magnitude of increase in E with increasing lithium content for binary vs Al-Cu-Li commercial aluminum-lithium alloys is unclear.

As shown in Section I of this report, increasing the lithium content of Weldalite™ 049 from 1.3 wt% to 1.9 wt% results in a 20% decrease in yield strength. It should also be noted that this increase in lithium results in about a 2% decrease in density. Thus, it appears that for most applications,

(3) Alloying, J.L. Walter, M.R. Jackson and C.T. Sims (eds)., ASM, Metals Park, OH (1988).
(4) K.K. Sankaran and N.J. Grant, Mater. Sci. Eng., 44, p. 213 (1980).

the decrease in strength would outweigh the benefits of increases in modulus associated with increasing the lithium level above 1.3 wt%.

As discussed in Section III of this report, the addition of approximately 4 v% TiB_2 to 049(1.3) results in an 8% increase in modulus. Clearly, further increases in modulus would accompany higher volume fractions of TiB_2, but the tendency for the particles to agglomerate would have to be overcome before the 049-TiB_2 could become a viable engineering alloy.

Report Documentation Page

1. Report No.	2. Government Accession No.	3. Recipient's Catalog No.
NASA CR-4364		

4. Title and Subtitle	5. Report Date
Microstructure-Property Relationships in Al-Cu-Li-Ag-Mg Weldalite™ Alloys	May 1991
	6. Performing Organization Code

7. Author(s)	8. Performing Organization Report No.
T.J. Langan J.R. Pickens	MML TR 90-27c
	10. Work Unit No. 505-63-50-02

9. Performing Organization Name and Address	11. Contract or Grant No.
Martin Marietta Laboratories 1450 S. Rolling Rd. Baltimore, MD 21227	NAS1-18531
	13. Type of Report and Period Covered: Contractor Report

12. Sponsoring Agency Name and Address	14. Sponsoring Agency Code
National Aeronautics and Space Administration Langley Research Center Hampton, VA 23665-5225	

15. Supplementary Notes

Langley Technical Monitor: William D. Brewer

Final Report - Part II

16. Abstract

The microstructure and mechanical properties of the ultrahigh strength Al-Cu-Li-Ag-Mg alloy Weldalite™ 049 were investigated during this phase of the research. Specifically, the microstructural features along with tensile strength, weldability, Young's modulus and fracture toughness were investigated for Weldalite™ 049-type alloys with Li contents ranging from 1.3 to 1.9 wt.%. The tensile properties of Weldalite™ 049 and Weldalite™ 049 reinforced with TiB_2 particles fabricated using the XD™ process were also evaluated at cryogenic, room, and elevated temperatures. In addition, an experimental alloy, similar in composition to Weldalite™ 049 but without the Ag+Mg, was fabricated. The microstructure of this alloy was compared with that of Weldalite™ 049 in the T6 condition to assess the effect of Ag+Mg on nucleation of strengthening phases in the absence of cold-work.

17. Key Words (Suggested by Author(s))	18. Distribution Statement
Al-Li Alloys, Metal Matrix Composites Weldalite™ 049, Elevated Temperature Al Alloy	Unclassified - Unlimited Subject Category 26

19. Security Classif. (of this report)	20. Security Classif. (of this page)	21. No. of pages	22. Price
Unclassified	Unclassified	98	A05

NASA FORM 1626 OCT 86

For sale by the National Technical Information Service, Springfield, Virginia 22161-2171

NASA-Langley, 1991

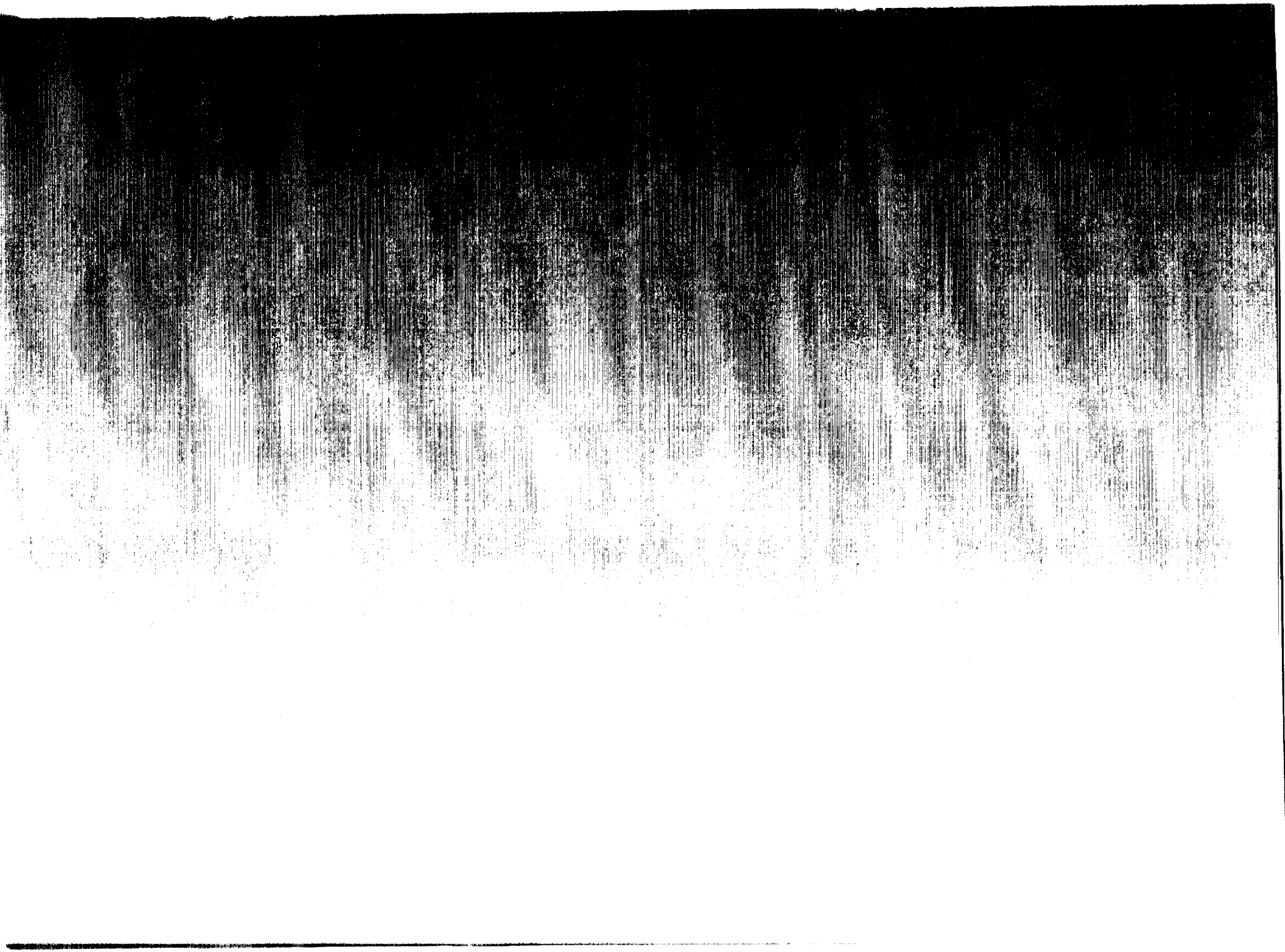

National
Space A
Op
Washing
20546-0

NA